

Published in final edited form as:

J Comp Neurol. 2011 August 15; 519(12): 2434–2474. doi:10.1002/cne.22635.

Vasopressin Innervation of the Mouse (*Mus musculus*) Brain and Spinal Cord

Benjamin D. Rood and Geert J. De Vries*

Center for Neuroendocrine Studies and Department of Psychology and Neuroscience, University of Massachusetts, Amherst, Massachusetts 01003

Abstract

The neuropeptide vasopressin (AVP) has been implicated in the regulation of numerous physiological and behavioral processes. Although mice have become an important model for studying this regulation, there is no comprehensive description of AVP distribution in the mouse brain and spinal cord. With C57BL/6 mice, we used immunohistochemistry to corroborate the location of AVP-containing cells and to define the location of AVP-containing fibers throughout the mouse central nervous system. We describe AVP-immunoreactive (-ir) fibers in midbrain, hindbrain, and spinal cord areas, which have not previously been reported in mice, including innervation of the ventral tegmental area, dorsal and median raphe, lateral and medial parabrachial, solitary, ventrolateral periaqueductal gray, and interfascicular nuclei. We also provide a detailed description of AVP-ir innervation in heterogeneous regions such as the amygdala, bed nucleus of the stria terminalis, and ventral forebrain. In general, our results suggest that, compared with other species, the mouse has a particularly robust and widespread distribution of AVP-ir fibers, which, as in other species, originates from a number of different cell groups in the telencephalon and diencephalon. Our data also highlight the robust nature of AVP innervation in specific regulatory nuclei, such as the ventral tegmental area and dorsal raphe nucleus among others, that are implicated in the regulation of many behaviors.

Keywords

lateral septum; immunohistochemistry; basal ganglia; amygdala; bed nucleus of the stria terminalis; dorsal raphe

The neuropeptide vasopressin (AVP) has become a key player in understanding the neurobiology of social behavior. Studies over the last 3 decades have suggested roles for AVP in behaviors such as social recognition, pair-bonding, partner preference, aggression, and communication in various species (Ferris et al., 1984; Dantzer et al., 1987, 1988; Dubois-Dauphin et al., 1989; Compaan et al., 1993; Insel et al., 1994; Lim et al., 2004; Lim and Young, 2004; Thompson et al., 2006), in addition to the physiological roles that AVP plays in regulating water balance, blood pressure, thermoregulation, and stress (Oliver and Schafer, 1895; Farini, 1913; Yates et al., 1971; Banet and Wieland, 1985; Naylor et al., 1985; Pittman and Franklin, 1985; Demotes-Mainard et al., 1986). Anatomical and pharmacological studies have identified several brain regions that are critical for AVP's effects on social behavior. For example, AVP facilitates and AVP antagonists inhibit territorial flank-marking in the hamster when injected into the anterior hypothalamus (Ferris

et al., 1984, 1986), pair-bond formation in the prairie vole when injected into the nucleus accumbens and ventral pallidum (Pitkow et al., 2001; Lim et al., 2004; Lim and Young, 2004), and social memory in the rat when injected into the lateral septum (Landgraf et al., 1995, 2003). These regions, however, are only a subset of those containing AVP-immunoreactive (-ir) fibers or AVP receptors.

The anatomy of the AVP system has been studied in more than 20 different mammalian species to date (De Vries and Panzica, 2006); however, a thorough accounting of the distribution of fibers throughout the brain has been made for only a select few, including the rat, guinea pig, macaque, and Brazilian opossum (DeVries et al., 1985; Caffè et al., 1989; Dubois-Dauphin et al., 1989; Iqbal and Jacobson, 1995). In most other studies, the authors focus on cell populations, fibers within distinct regions of the brain, or subset of areas with the densest innervation (e.g., the lateral septum, lateral habenula, and medial amygdala). In nearly every species examined, including the mouse (Castel and Morris, 1988; Abrahamson and Moore, 2001; Ho et al., 2010), AVP neurons are found in the same five brain regions: the paraventricular hypothalamus, suprachiasmatic nucleus, supraoptic nucleus, bed nucleus of the stria terminalis (BNST), and medial amygdala. Most species also have AVP-producing cells dispersed over the hypothalamus. Presumably, these cell groups contribute to the numerous AVP-ir fibers and terminals found throughout the brain. Where they have been examined, AVP-ir fiber patterns are also relatively similar between species, although only a few species have been directly compared, for example, the prairie and meadow vole (Bamshad et al., 1993) and the white-footed and California mouse (Bester-Meredith et al., 1999). However, a number of interesting species differences do exist. For example, the golden hamster lacks AVP-producing cells in the BNST and medial amygdala and AVP fibers in the lateral septum (Dubois-Dauphin et al., 1990; Albers et al., 1991; Ferris et al., 1995; Miller et al., 1999), which is thought to receive its innervation from the BNST and medial amygdala (De Vries and Buijs, 1983; Caffè et al., 1987). Another extreme example is the naked mole rat, which lacks AVP-producing cells in the suprachiasmatic nucleus (SCN) and AVP fibers in the subparaventricular zone and dorsomedial hypothalamus, which are thought to be innervated by the SCN in other species (Hoorneman and Buijs, 1982; Rosen et al., 2007).

Recently, the mouse has become one of the premier model organisms for studying behavioral neuroscience because of advances in transgenic technology. Studies manipulating the AVP system, specifically the V1a and V1b AVP receptors, have provided a number of insights into the function of the AVP system in the mouse. For instance, a null mutation of the V1a receptor, the most prevalent AVP receptor in the brain (Ostrowski et al., 1992, 1994; Saito et al., 1995), disrupts social recognition; knockout mice investigate novel and familiar females to a similar extent, whereas wild-type mice spend less time investigating a familiar female (Bielsky et al., 2004). Null mutations of the V1b receptor reduce aggression; knockout mice have a longer attack latency and reduced attack frequency than wild-type littermates (Wersinger et al., 2002). Finally, changing the species-typical pattern of V1a AVP receptor distribution in the brains of mice by replacing the mouse V1a receptor gene with a V1a receptor transgene, including the promoter region, from the highly social prairie vole resulted in increased affiliative behaviors (Young et al., 1999). These types of studies break new ground in the understanding of AVP function using mouse models.

In contrast, knowledge of AVP peptide location in the mouse brain remains incomplete. Previous work has provided a detailed account of the various AVP-ir cell groups, including measurements of cell size and the characteristics of fibers in the forebrain but not the midbrain, hindbrain, or spinal cord (Castel and Morris, 1988; Abrahamson and Moore, 2001; Ho et al., 2010), nor do any studies provide a detailed analysis of distribution of fibers in structures such as the amygdala and basal ganglia, where AVP has important effects on

social behavior (Pitkow et al., 2001; Lim and Young, 2004). A more detailed profile of AVP immunoreactivity is crucial for forming hypotheses regarding AVP function in the brain, especially as more and more data are compiled on the unique contribution of very distinct brain regions to various neural processes, including those inherent to social behaviors.

This article describes the distribution of AVP-ir fibers and cell bodies throughout the central nervous system of male C57BL/6 mice. In our descriptions of the telencephalon and diencephalon, we corroborate previous research as well as provide a detailed subregion analysis not previously carried out. In addition, we provide for the first time a description of AVP-ir fiber distribution in the midbrain, hindbrain, and spinal cord of the mouse central nervous system.

MATERIALS AND METHODS

Animals

Eighteen male sexually inexperienced C57BL/6 mice were obtained from a breeding colony at the University of Massachusetts at approximately 120 days of age. Throughout the duration of the experiment, animals were group housed at weaning (five or fewer per cage) with same-sex siblings under a 14:10-hour light cycle with lights on at 6:00 AM. Animals had ad libitum access to food and water. All procedures conformed to National Institutes of Health guidelines and were in accordance with a protocol approved by the University of Massachusetts Institutional Animal Care and Use Committee.

Tissue collection and processing

Brain—Brains from three mice were used for the detailed descriptive analysis of the distribution of AVP-ir fibers in the brain. The brains of 12 other males were used to corroborate the observations made in this study. Mice were killed by CO₂ asphyxiation, followed by rapid decapitation. Brains were removed rapidly and placed in 5% acrolein (Sigma Aldrich, St. Louis, MO) in 0.1 M sodium phosphate buffer, pH 7.6 (PBS), for 4 hours, after which brains were transferred to 30% sucrose in PBS and stored at 4°C until sectioning. Brains were sectioned at 30 μm in one of three planes: coronal, sagittal, or horizontal. For each brain, every other section was collected for AVP immunohistochemistry. All brain sections for immunohistochemistry were stored in cryoprotectant at –20°C until staining. Alternate sections were briefly stored in 0.05 M Tris-buffered saline until being mounted on slides and Nissl stained. For animals used to corroborate results of this study, only every third coronal section (30 μm sections) was collected for AVP immunohistochemistry.

Hindbrain and spinal cord—An additional three male mice were killed with an overdose of pentobarbital, followed by intracardial perfusion with 50 ml 0.9% saline, followed by 50 ml of 5% acrolein in 0.1 M PB. Brains and spinal cords were removed after perfusion and stored in 5% acrolein in 0.1 M PB for 4 hours and then switched to 30% sucrose in 0.1 M PB. Brains and spinal cords were stored in sucrose until sectioning. Hindbrains were blocked from the forebrain, and every third section was collected for AVP immunohistochemistry. One spinal cord was sectioned in the coronal plane. Every other section (40-μm sections) was collected for AVP immunohistochemistry. The remaining two spinal cords were cut along the sagittal plane (30-μm sections), and every other section was collected for AVP immunohistochemistry. For the coronal series and one of the sagittal series, alternate sections were collected for Nissl staining.

Nissl staining

Alternate brain sections not stained for AVP were mounted onto gelatin-coated slides and allowed to dry overnight. Sections were rinsed for 2×2 minutes in purified water and then for 2×2 minutes in 70% ethanol, followed by a 5-minute incubation in thionin. Sections were rinsed in purified water and placed in 70% ethanol plus 0.1% glacial acetic acid for 10 minutes. Sections were dehydrated in 95% ethanol (1 minute) followed by 100% ethanol (2×1 minute) and finally rinsed in Hemo-De (Scientific Safety Solvents, Kellar, TX) for 4 minutes prior to coverslipping.

Immunohistochemistry

Immunohistochemistry was carried out in Netwell mesh-bottomed cups (15-mm-diameter cups with 74- μ m mesh; Corning, Corning, NY), and all incubations and rinses were performed at room temperature except where otherwise noted. Sections were incubated in the following solutions: 3×5 minutes in Tris-buffered saline (TBS; 0.05 M Tris, 0.9% NaCl, pH 7.6); 30 minutes in 0.05 M sodium citrate in TBS; 3×5 minutes in TBS; 30 minutes in 0.1 M glycine in TBS; 3×5 minutes in TBS; and 30 minutes in blocking solution [20% normal goat serum (NGS), 0.3% Triton X (Labchem, Pittsburgh, PA) and 1% H_2O_2 in TBS]. Sections were transferred to 2-ml centrifuge tubes containing primary antiserum [2% NGS, 1% BSA, 0.3% Triton X, and 1:12,000 guinea pig anti-AVP antiserum (T-5048; Peninsula Laboratories, San Carlos, CA)]. After incubating overnight (~18 hours), sections were returned to wells and rinsed with TBS containing 1% NGS and 0.02% Triton X for 3×10 minutes at 37°C. Next, sections were incubated in secondary antiserum [1:250 biotinylated goat anti-guinea pig IgG (Vector Laboratories, Burlingame, CA) in TBS with 2% NGS and 0.32% Triton X] for 1 hour, followed by 3×10 minutes rinses in TBS containing 0.2% Triton X. Sections were then incubated for 1 hour in avidin-biotin complex in TBS (ABC Elite kit; Vector Laboratories), followed by 3×10 minute rinses in TBS. Sections were incubated in DAB with nickel enhancer as per kit instructions (DAB peroxidase substrate kit; Vector Laboratories) for 2.5 minutes, followed by 4×5 minute rinses in TBS. Sections were mounted on gelatin-coated slides and allowed to dry at least overnight. Sections were subsequently rinsed for 3×30 seconds with purified water and allowed to dry before being coverslipped using Permount (ThermoFisher Scientific, Waltham, MA)

Antibody characterization

The AVP antiserum (T-5048) recognizes the nine-amino-acid peptide (Arg⁸)-AVP (H-Cys-Tyr-Phe-Gln-Asn-Cys-Pro-Arg-Gly-NH₂) and was raised against a synthetic peptide. This antibody has minimal cross-reactivity with (Lys⁸)-AVP or oxytocin, another nonapeptide as determined by radioimmunoassay (manufacturer's data sheet). No immunostaining was seen in control sections in which the antiserum was omitted or in sections in which the antiserum was preadsorbed with 50 μ M (Arg⁸)-AVP (Sigma Aldrich) at room temperature for 1 hour prior to overnight tissue incubation. Preadsorption with 50 μ M oxytocin (Sigma Aldrich) did not block immunostaining.

Analyses and image acquisition

Observations were made with a brightfield microscope (Nikon Eclipse E600; Nikon Instruments, Melville, NY). Nissl-stained sections were used for reference. Photomicrographs were taken with a MicroFire camera and Picture-Frame software (Optronics, Goleta, CA). Anatomical nomenclature and regional delineation were according to Franklin and Paxinos (2008). Photomicrographs were adjusted for contrast and brightness.

RESULTS

Cells in the telencephalon

BNST—Outside of the hypothalamus, AVP-ir cells were only found in the BNST and medial amygdala (MeA). In the BNST, most of the cells observed are small (i.e., parvocellular), very lightly staining, and found primarily in two subdivisions of the BNST. The first group of cells is located in the medial posteromedial BNST (BSTMPM) just lateral to the fornix and medial to fibers entering from the stria terminalis (Fig. 1A,C). A second, more diffuse, cluster of cells is observed caudally in the lateral posteromedial BNST (BSTMPL). This cell group spreads out in a dorsolateral to ventromedial orientation starting just ventral to the stria terminalis (Fig. 1B,D). Aside from these two locations, a few lightly staining small cells are scattered throughout the posterior BNST, and a few isolated cells are observed in the anteromedial BNST. Finally, occasional large, darkly staining neurons are observed in both the BSTMPM and the BSTMPL.

MeA—A smaller and more loosely organized collection of AVP-ir cells is found in the MeA. These cells, like those in the BNST, are small and stain very lightly. They typically appear from rostral to caudal levels of the posterodorsal medial amygdala (MePD) and tend to concentrate on the lateral edge of this nucleus (Fig. 1E–H).

Cells in the diencephalon

Paraventricular nucleus—The paraventricular (PVN), supraoptic (SON), and suprachiasmatic (SCN) nuclei contain the three largest concentrations of AVP-ir cells in the hypothalamus. The most rostral part of the PVN begins just caudal to the decussation of the anterior commissure. Here, only a few large, darkly staining cells are observed just ventral to the dorsal tip of the third ventricle in the anterior parvocellular PVN (Fig. 2A). Caudally, the number of cells increases dramatically along the dorsal half of the ventral third ventricle in the ventral (PaV) and medial magnocellular PVN (Fig. 2B). Subsequently, a group of AVP-ir cells appears laterally in the lateral magnocellular PVN (PaLM) near the dorsal tip of the third ventricle, the PaV cell group ends, and a less dense group of immunoreactive cells is seen in the medial parvocellular PVN (PaMP; Fig. 2C). Caudally, the labeling in the PaLM cell group continues to be dense, but fewer labeled cells are observed adjacent to the third ventricle in the PaMP (Fig. 2D). As the fornix nears the dorsal–ventral midline of the third ventricle, the PVN ends with just a few scattered AVP-ir cells near the dorsal edge of the ventricle.

Supraoptic nucleus—The distribution of AVP-ir cells in the supraoptic nucleus (SON) is rather extensive. Large, darkly staining cells first begin to appear hugging the ventral surface of the brain just dorsal and lateral to the optic chiasm in the episupraoptic nucleus (Fig. 2E). As the optic tract curves up into the brain, large, darkly staining cells are so densely packed at the dorsal aspect of the optic tract that they often cannot be distinguished (Fig. 2F). Although most AVP-ir cells in the SON are seen in a distinct cluster just dorsal and lateral to the optic tract, a string of large cells spreads medially immediately dorsal to the optic tract, stopping in the retrochiasmatic region ventral to the anterior hypothalamus (rostrally) and ventromedial hypothalamus (caudally; Fig. 2G). As the optic tracts take a sharp turn dorsally to meet the cerebral peduncles, the large AVP-ir neurons of the SON disappear (Fig. 2H).

Suprachiasmatic nucleus—The suprachiasmatic nucleus (SCN) contains a very dense cluster of small, darkly staining cells, which at times are difficult to tell apart because of an extremely dense halo of fibers and terminals surrounding the nucleus. AVP-ir cells in the SCN form a shell around a core that is nearly devoid of AVP-ir cells. Densely packed cells are found in the rostral (Fig. 3A) and caudal (Fig. 3C) poles. In the middle of the SCN,

AVP-ir cells form a shell dorsal, lateral, and medial to an AVP-ir-sparse central core. The ventral part contains fewer cells (Fig. 3B).

Accessory nuclei—In addition to the AVP-ir cells of the above-mentioned nuclei, numerous other cells are scattered throughout the hypothalamus. Because many of these appear similar in size and shape to magnocellular neurons of the PVN and SON and lie along fiber pathways from these nuclei, these cells are often referred to as *accessory nuclei* (Krisch, 1976). The accessory cells are most consistently found in the anterior hypothalamus (AHA; Fig. 4A), perifornical region (Fig. 4B), and peduncular lateral hypothalamus (PLH; Fig. 4C). In addition, a loosely packed cluster of AVP-ir cells is located rostral to the PVN, just ventral to the fornix in the striohypothalamic region (StHy; Fig. 4D); this cell group is referred to as the *mouse accessory nucleus* by Castel and Morris (1988).

Other hypothalamic nuclei—First, a small but particularly dense cluster of AVP-ir cells is observed in the nucleus circularis (Fig. 4E). Second, scattered neurons are seen in rostral parts of the periventricular area (Fig. 4F). Third, AVP-ir cells are found in the ventral lateral preoptic area where they cluster tightly along the ventral brain surface (Fig. 4G). It is unclear whether this group is an extreme rostral extension of the supraoptic nucleus or a separate group of AVP-ir cells. Finally, a dense cluster of cells is observed caudal to the last SON cells along the ventral surface of the brain in the retrochiasmatic supraoptic nucleus (Fig. 4G). These cells can be difficult to see as they are buried in a dense tangle of AVP-ir fibers passing through the tuberal lateral hypothalamus.

Small vs. medium-sized fibers

Throughout the descriptions of AVP-ir fibers below, we refer to *small* and *medium-sized* fibers. In general, the characteristics of fibers provide a unique insight into various fiber pathways. In rats, medium-sized fibers are typical of projections deriving from neurons in the PVN (De Vries and Buijs, 1983) and associated neurons. In contrast, small fibers are typical of projections from the BNST, MeA, and SCN (Buijs et al., 1978; De Vries and Buijs, 1983). Small fibers typically have thin processes with small varicosities as seen in the lateral septum (LS; Fig. 5A; see also Fig. 8F). In addition, small fibers are almost always associated with scattered punctate staining, which is thought to indicate synaptic terminal fields (Buijs and Swaab, 1979). In contrast, medium-sized fibers are larger, have larger varicosities, and often stain more darkly. In addition, these fibers are rarely associated with the small punctate staining typical of small fiber terminal fields. Instead, these fibers have occasional visible protrusions, possibly terminal boutons, that branch off the fiber as it passes through an area as in the ventral periaqueductal gray (VLPAG; Fig. 5B). A list of the brain areas described below along with their relative AVP-ir fiber densities is provided in Table 1. In our descriptions, our use of the term *medium-sized* includes large fibers, which are found mainly at the ventral base of the hypothalamus and surrounding AVP-ir neurons of the supraoptic nucleus. These large fibers are probably dendrites of magnocellular neurons (Castel and Morris, 1988; Ludwig and Leng, 2006). Because the distinction between large and medium-sized fibers is not as clear as the difference between small and medium-sized fibers, we acknowledge that our designation *medium-sized* likely includes multiple types of fibers, including some dendrites.

Fibers in the telencephalon

Cortex—Most of the cortex is devoid of AVP-ir fibers, although a few exceptions exist. In the frontal lobe, isolated medium-sized fibers are observed in midline cortical nuclei such as the medial orbital, frontal, infralimbic, prelimbic (PrL; Fig. 6A), and dorsal peduncular cortex. The insular cortex just dorsal to the rhinal fissure contains sparse fibers at points along its rostral to caudal length (Fig. 6B). The rostral cingulate cortex (Cg2) also contains a

very sparse innervation, often only a single fiber (Fig. 6C). The densest innervation of the cortex occurs caudally as the hippocampus curves toward the ventral brain surface, where small AVP-ir fibers form diffuse plexuses in the endopiriform, entorhinal, intermediate endopiriform claustrum, and dorsolateral entorhinal cortex (DLEnt; Fig. 6D).

Hippocampus—Dorsally, the hippocampus is devoid of AVP-ir fibers, and only a rare fiber is observed in the fimbria. In contrast, as the hippocampus joins the caudal amygdala, small fibers are observed in the oriens layer (Or) of the hippocampus and along the border between the hippocampal formation and the amygdala-hippocampal transition zone (AHiPM; Fig. 6E,F) and farther caudally in the ventral subiculum and molecular layer of CA1. Medium-sized fibers are observed in the caudal molecular layer of CA1 (Fig. 6G,H).

Basal ganglia—The caudate, putamen, and globus pallidus do not contain AVP-ir fibers. The nucleus accumbens contains medium-sized fibers mostly in its core region (AcbC; Fig. 7A,B). The ventral pallidum (VP), however, contains many small fibers and terminals. Rostrally, there are densely innervated patches of VP between the shell of the nucleus accumbens (AcbSh) and the olfactory tubercle (Tu), neither of which contains labeled fibers (Fig. 7A). As the vertical limb of the diagonal band (VDB) becomes prominent, the dense patches of fibers in the VP seem continuous with a dense band of AVP-ir fibers between the diagonal band and the accumbens shell. As the horizontal limb of the diagonal band (HDB) begins to spread laterally, the VP contains a less dense innervation located primarily in the medial portion of the VP ventral to the waning nucleus accumbens (Fig. 7B). The central region of the VP does not contain AVP-ir fibers at this level, and, caudally, the innervation of the ventral pallidum becomes increasingly sparse.

Ventral forebrain—Rostral to the diagonal band, there are AVP-ir fibers along the midline in the navicular postolfactory nucleus. These fibers extend up into the intermediate lateral septum (LSI), avoiding the shell of the nucleus accumbens. As the diagonal band emerges, a dense band of small fibers stretches dorsally from the ventral surface toward the septal region between the diagonal band (VDB) and nucleus accumbens and around the islands of Calleja (ICjM), all of which are devoid of fibers (Fig. 7A). This region containing dense fibers is unnamed in *The mouse brain in stereotaxic coordinates* (Franklin and Paxinos, 2008) but corresponds to the ventral septal area (VSA) described by Naylor et al. (1985) and is not to be confused with the ventral lateral septum (LSV). Rostrally, pockets of AVP-ir fibers in the ventral pallidum are continuous with this fiber plexus (Fig. 7A), and caudally fibers spread into the substantia innominata (SI; Fig. 7B).

Septal complex—The rostral septum contains sparse medium-sized fibers in all three divisions (ventral, intermediate, and dorsal; LSV, LSI, LSD; Fig. 8A). Caudally, as the anterior commissure (ac) becomes plumb with the ventral edge of the lateral ventricle, small fibers spread dorsally along the lateral edge of the diagonal band in the ventral septal area, invading the ventral lateral septum (LSV), intermediate lateral septum (LSI), and to a lesser extent the septohypothalamic nucleus (SHy; Fig. 8B). The plexus of small fibers becomes very dense in the ventral and intermediate lateral septum as the fibers of the fimbria become visible (Fig. 8C). In this region, pericellular baskets, distinct clusters of immunoreactivity that appear to surround individual cells, are observed (Fig. 8E,F). At the caudal extent of the septal complex (Fig. 8D), some small fibers make their way into the fringes of the septofimbrial region (SF_i), although the main body of the fimbria is devoid of AVP-ir fibers. The dorsal lateral septum (LSD) contains only an occasional medium-sized fiber. In sharp contrast to the lateral septum, the medial septum (MS) does not contain AVP fibers (Fig. 8A,B). However, medium-sized fibers rise up just lateral to the medial septum and occupy a region between the medial septum and the dense plexus of small fibers of the lateral septum.

In addition, medium-sized fibers pass through the median preoptic area rostral to the anterior commissure and ascend into the subfornical organ (SFO; Fig. 8D). A few fibers reach the triangular septal nucleus as well.

BNST—Each division of the BNST presents a unique pattern of AVP-ir fibers. In the anterior BNST, just caudal to the nucleus accumbens (Fig. 9A), medium-sized fibers are found both dorsal and ventral to the anterior commissure in the anteromedial (BSTMA) and medioventral (BSTMV) divisions. The lateral nuclei dorsal and ventral to the anterior commissure contain only isolated, medium-sized fibers. At this rostral level, the BSTMA also contains small fibers. As the anterior commissure decussates (Fig. 9B), a dense plexus of medium-sized fibers is observed in the BSTMV ventral to the decussation. At this level, the BSTMA has an increased density of small fibers. The dorsal lateral nuclei still contain almost no fibers, but small fibers begin to appear in the ventral lateral region.

In the posterior BNST, the medial part of the posteromedial nuclei (BSTMPM) contains a dense plexus of small fibers just dorsal to the stria terminalis and another less dense plexus closer to the dorsal edge of the nucleus, adjacent to the dorsal third ventricle (Fig. 9C). The center of the BSTMPM contains a moderate amount of small fibers. The intermediate (BSTMPI) and lateral (BSTMPL) posterior BNST contains small AVP-ir fibers as well (Fig. 9D,E). Many small fibers appear to travel dorsally into the stria terminalis and laterally into the extended amygdala¹ (EA) from the posterior BNST. Caudal to the posterior BNST, small fibers persist ventral to the stria medullaris and lateral to the fornix (Fig. 9E).

Amygdala—The amygdala is made up of multiple distinct cell groups, only some of which contain AVP immunoreactivity. Rostrally, the EA contains small fibers, some of which extend into the anterior amygdaloid nucleus (AA; Fig. 10A,B). The anterior cortical amygdala (ACo) also contains a light AVP-ir innervation. Fibers do not make their way into the piriform cortex, cortex–amygdala transition zone, basolateral amygdala, lateral olfactory tract (LOT; Fig. 10C,D), bed nucleus of the accessory olfactory tract, or magnocellular preoptic area. At the rostrocaudal level of the anterior amygdala, small fibers are found in both dorsal and ventral parts of the anterior MeA, basomedial amygdala, and ventral basolateral amygdala. Some fibers reach the endopiriform cortex at this point as well.

Caudally, the posterodorsal (MePD) and posteroventral medial amygdala replace the anterior medial nuclei along the optic tract and contain dense small fibers. In fact, the MePD has the densest fiber concentration of the entire amygdala (Fig. 10F) and is the only nucleus in this region with pericellular baskets similar to those observed in the lateral septum (see Fig. 8F). Caudal to the MePD, AVP-ir fibers decrease in number. Some small fibers are seen in the posterolateral cortical amygdala, between the caudal lateral (LA) and the posterior basolateral amygdala (BLP; Fig. 10G,H), and in the amygdalohippocampal area (AHiPM; see Fig. 6F). Although most AVP-ir fibers in the amygdala are small, sparse medium-sized fibers are seen in the MeA, basomedial amygdala, and ventral endopiriform nucleus. The densest group of medium-sized fibers, however, is seen in the central nucleus of the amygdala, which does not contain small fibers at all (CeM; Fig. 10E).

¹For consistency, we use the terminology used in *The mouse brain in stereotaxic coordinates, 3rd ed* (Franklin and Paxinos, 2008). However, the term *extended amygdala* is usually used to refer to a group of interconnected brain regions including the central and medial amygdala and the BNST and includes the area called *extended amygdala* in this article (de Olmos and Heimer, 1999). In *The rat brain in stereotaxic coordinates* (Paxinos and Watson, 1998), this area between the globus pallidus and peduncular lateral hypothalamus is considered to be part of the substantia innominata.

Fibers in the diencephalon

Hypothalamus: preoptic area—The preoptic region is marked by a rich innervation of both small and medium-sized AVP-ir fibers. In the rostral pole of the preoptic area, the medial preoptic area (MPA) and lateral preoptic area (LPO) contain small fibers. More caudally, the vascular organ of the lamina terminalis (VOLT) and the median preoptic nucleus (MnPO) at the midline contain mostly medium-sized fibers (Fig. 11A,B). Fibers in the latter structure appear to pass dorsally into the septal region (Fig. 11B). At the decussation of the anterior commissure, there is a dense plexus of small AVP-ir fibers in the parastrial nucleus (PS; Fig. 11C), immediately medial to a cluster of medium-sized fibers in the ventral BNST. Ventrally, the medial part of the preoptic nucleus (MPOM) contains mostly small fibers, although some medium-sized fibers stray from the midline periventricular nuclei into this area. The midline regions including the anteroventral periventricular nucleus (AVPe), periventricular nucleus (Pe), and ventromedial preoptic area (VMPO) contain many small and medium-sized fibers (Fig. 11D,E).

Hypothalamus: anterior hypothalamus—In this region, small fibers are found almost exclusively near the midline except at the most anterior part of the anterior hypothalamus (AHA), where small AVP-ir fibers are observed just below the fornix. At the midline, a dense cloud of small fibers surrounds the AVP-ir cells of the SCN and spreads dorsally into the subparaventricular zone (SPa) and periventricular area (Pe), forming the densest plexus of small fibers seen anywhere in the brain (Fig. 12A–C). Only a few small fibers stray into the anterolateral hypothalamus and caudal AH. In contrast, many small fibers appear to enter and pass through the PVN. Sagittal sections of the SCN reveal small fibers travelling in multiple trajectories, with the densest projections oriented rostradorsal, dorsal, and caudodorsal from the SCN (Fig. 13B).

Medium-sized fibers in the AH are found in three major medial to lateral pathways. The first bundle of fibers appears to leave the rostral aspect of the ventral PVN (PaV) and pass ventrolaterally toward the edge of the optic chiasm (Fig. 12A). These fibers are joined by fibers from a number of accessory cells located in the AH. The second group exits the PVN more dorsally and takes a ventrolateral route just below the fornix (Fig. 12B). The third group of fibers, which extends the farthest caudally (Fig. 12C), passes over the dorsal edge of the fornix, splitting into ventral and dorsal paths. The dorsal path turns dorsally into the reticular nucleus of the thalamus, whereas the ventral path turns toward the SON. Both dorsal and ventral routes pass accessory cells whose fibers seem to join the other fibers. Finally, dense networks of small, medium-sized, and large fibers crisscross the midline periventricular region along the length of the third ventricle (Fig. 13A).

Hypothalamus: dorsomedial hypothalamus—Caudal to the PVN, the dorsomedial hypothalamus (DM) contains small fibers, which stay close to the ventricle rostrally (Fig. 14A), but spread laterally almost to the fornix caudally (Fig. 14B,C). Where the small fibers spread laterally, several medium-sized fibers appear to spread medially into the lateral DM (Fig. 14C). At the level of the DM, the ventromedial hypothalamus (VMH) is nearly devoid of fibers, although, ventral to the fornix and the rostral VMH, dense collections of medium-sized fibers forge a path toward the median eminence (Fig. 14A,B). Caudally, these fibers form a thin sheet as they reach the median eminence, where most fibers are concentrated in the inner zone, with a less dense plexus extending in the highly vascularized region of the outer zone (Fig. 14D). Finally, near the ventral midline, small fibers are found in the retrochiasmatic area rostrally, the arcuate nucleus (Arc; Fig. 14D) caudally, and the periventricular nucleus throughout.

Hypothalamus: lateral hypothalamus—The emergence of the peduncular lateral hypothalamus (PLH) caudal to the lateral preoptic area is marked by an increase in density of small AVP-ir fibers (Figs. 12A–C, 15A). These fibers occur in a large cloud over much of the lateral hypothalamus from the fornix medially to the sublenticular portion of the extended amygdala (a.k.a., substantia innominata; see footnote 1) laterally and ventrally around the horizontal diagonal band, which is devoid of fibers. Caudally, small fibers in the PLH become less dense and finally quite sparse. At the same level, there is an increase in medium-sized fibers, which, based on their trajectory, appear to be associated with the PVN, SON, and accessory nuclei (Fig. 15B).

Hypothalamus: mammillary bodies—The mammillary nuclei (MB), which are found caudal to the DM, are completely devoid of AVP-ir fibers. In contrast, just rostral to the mammillary nuclei, a lateral to medial band of small fibers that surrounds the fornix stretches from the lateral edge of the brain almost to the midline in the perifornical lateral hypothalamus (PeFLH; Fig. 15C). Dorsal and ventral to this band of fibers, medium-sized fibers are observed in the ventral premammillary (PMV), posterior hypothalamic (PH), and parasubthalamic nuclei (PSTh; Fig. 15C). The dorsal (DTM) and ventral (VTM) tuberomammillary nuclei are both innervated by small fibers (Fig. 15C–E). Ventral to the increasingly prominent mammillary nuclei, small and medium-sized fibers are pushed ventrally (Fig. 15D) until only the dense innervation of the VTM remains (Fig. 15E); dorsal to the mammillary nuclei, the retromammillary nuclei (RMM) contain some small and medium-sized fibers (Fig. 15D,E).

Thalamus—With the exception of a few medium-sized fibers in the reticular, paraventricular, reuniens, and xiphoid nuclei, the thalamus is innervated by small AVP-ir fibers. Along the dorsal midline of the thalamus, small fibers are found from the rostral anterior paraventricular nucleus (PVA) to the caudal paraventricular nucleus (PV), which ends just rostral to the posterior commissure. In the PV, small fibers are concentrated rostrally (Fig. 16A) and become scarce in more caudal regions (Fig. 16B–D,G).

A second plexus of fibers extends along a path similar to that in the PV but lies laterally on either side of the PV. Rostrally, small fibers are observed just dorsal to the much less densely innervated paratenial nucleus (Fig. 16A). This fiber plexus continues caudally into the rostral tip of the mediodorsal thalamus (MD; Fig. 16B,C). Continuous with fibers in the mediodorsal thalamus is a collection of fibers that invades midline nuclei ventral to the PV, most prominently, the centromedial nucleus (CM), rhomboid nucleus (Rh), and intralaminar nuclei, including the paracentral (PC), interanterodorsal, and interanteromedial (IMD) nuclei (Fig. 16B–D). Caudally, this lateral fiber plexus concentrates dorsally in the lateral habenula (LHb), in sharp contrast to the adjacent and empty medial habenula (Fig. 16D,G). A sagittal view shows the lateral fiber plexus travelling dorsally parallel to the stria medullaris (sm) with concentrations of small fibers in the MD and LHb (Fig. 16H). Figure 16F,G shows coronal views of the MD and LHb, respectively.

In the ventral thalamus, small AVP-ir fibers pass through the densely innervated paraventricular nucleus to innervate the xiphoid nucleus (Xi; Fig. 16E) and to a lesser extent the paraxiphoid (PaXi) and reuniens nuclei (Re). These fibers do not extend dorsally into the other midline nuclei, such as the rhomboid nucleus. Finally, a light innervation of small fibers is located in the zona incerta above the fornix (Fig. 16I).

Fibers in the mesencephalon

Tectum—The tectum (i.e., superior and inferior colliculi) is nearly devoid of fibers with the exception of a small pocket of small fibers observed at the midline within and above the

commissure of the superior colliculus at the same level where small fibers and terminals are found in the dorsomedial periaqueductal gray (described below).

Tegmentum—Rostrally, small fibers populate the ventral tegmental area (VTA), pigmented parabrachial nucleus of the VTA (PBP), and interfascicular nucleus (IF) caudal to the mammillary bodies (Fig. 17A). Caudally, small fibers are found throughout the IF and parainterfascicular (PIF) nuclei (Fig. 17B). In addition, small fibers spread laterally into the anteroventral tip of the substantia nigra pars reticulata (SNR; Fig. 17A) and farther laterally into the substantia nigra pars compacta (Fig. 17B). Other prominent nuclei such as the rostral interpeduncular nucleus (IPR) and red nucleus (RMC) do not contain any fibers (Fig. 17B). The mRT also shows a plexus of small fibers (Fig. 17C). Medium-sized fibers are found in most of these areas as well. In fact, a prominent medium-sized fiber pathway passes dorsal to the substantia nigra through the parasubthalamic nucleus and zona incerta; these fibers appear to consolidate into a denser plexus in a somewhat ambiguous area where the caudal lateral part of the substantia nigra, subbrachial nucleus (SubB), and midbrain reticular formation (mRT) come together (Fig. 17C). A smaller plexus of medium-sized fibers is seen in the retrorubral field (RRF) as well. Farther caudally, some medium-sized fibers travel dorsally and medially toward the medial parabrachial nucleus. As pontine regions begin to overtake the tegmentum, some small AVP-ir fibers pass from the interfascicular nucleus into the caudal linear raphe nucleus (CLi; Fig. 17D), whereas others wrap around the rostral interpeduncular nucleus to enter into the caudal interpeduncular nucleus (IP; Fig. 17E).

Periaqueductal gray and dorsal raphe nuclei—Both small and medium-sized fibers appear to enter the periaqueductal gray (PAG) and dorsal raphe (DR) nuclei from two distinct paths, which can be seen in sagittal sections taken near the midline (Fig. 18A). The first pathway is through the midbrain tegmentum just caudal to the posterior hypothalamus (Fig. 18A,B), and the second is through the interfascicular nuclei (IF) and caudal linear raphe (CLi). These regions contain small and medium-sized fibers that are elongated without the punctate staining or terminal boutons that are typically associated with small and medium-sized fibers and therefore resemble fibers of passage. Within the PAG, a plexus of small fibers is observed in the dorsomedial PAG (DMPAG), which spreads laterally into the dorsolateral PAG, but occupies only the rostral pole of the PAG (Fig. 18C,D). The remainder of the PAG contains a few medium-sized fibers, although most fibers appear to travel parallel to the cerebral aqueduct and are best seen in sagittal sections (Fig. 18A). In the caudal PAG, many medium-sized fibers turn laterally into the ventrolateral PAG (VLPAG), whereas others turn dorsally into the caudal DMPAG (Fig. 18I,J). Many of the ventral fibers appear to continue into the lateral parabrachial nucleus.

At the level of the trochlear nucleus (4N) in the rostral pole of the DR, a plexus of small fibers emerges on either side of the midline in the dorsolateral dorsal raphe (DRL; Fig. 18E,F). Caudally, the small fibers converge to form a very dense plexus at the midline in the dorsal part of the DR (DRD; Fig. 18G,H). As the laterodorsal and dorsal tegmental nuclei, which do not contain AVP-ir fibers, become more prominent, the caudal DR (DRC) is pressed into the midline, where small fibers are found (Fig. 18I).

Caudal mesencephalic nuclei—Some medium-sized fibers appear to pass into the lateral parabrachial nucleus (LPB) via the caudal ventrolateral PAG (Fig. 19A). At the same level, medium-sized fibers are seen in the medial parabrachial nucleus (MPB; Fig. 19A), which appear to be continuous with fibers passing through the midbrain reticular formation from more ventral regions. Caudally, the locus coeruleus (LC) and Barrington's nucleus (Bar) both contain medium-sized fibers (Fig. 19B). Caudal to the lateral parabrachial nucleus, locus coeruleus, and Barrington's nucleus, all remaining fibers appear to travel

caudally adjacent to the ventricle and do not spread out into the coronal plane until the myelencephalon.

Fibers in the metencephalon

Very few AVP-ir fibers are found in the metencephalon. The cerebellum, deep cerebellar nuclei, vestibular nuclei, pontine nuclei, and pontine reticular formation are devoid of fibers. However, small fibers are found in the median raphe (MnR; Fig. 20A). Adjacent to the median raphe on either side, a small but notable plexus is observed in the anterior tegmental nucleus (ATg; Fig. 20B). The subcoeruleus and intermediate reticular formation contain sparse medium-sized fibers (IRt; Fig. 20C).

Fibers in the myelencephalon

Dorsal myelencephalon—Stretching caudally from the midbrain reticular formation, sparse medium-sized AVP-ir fibers are found in the alpha part of the parvocellular reticular formation beneath the vestibular nuclei just rostral to the solitary nucleus. Medium-sized fibers collect in the solitary nucleus (Sol; Fig. 20D,E), forming a dense plexus, which, although visible in coronal sections, is best seen in sagittal sections (Fig. 20F,G). These fibers are restricted to the solitary nucleus and to a lesser extent the nucleus of the vagus. They do not enter ventrally into the hypoglossal nucleus (12N; Fig. 20G). Some fibers continue toward the back of the solitary nucleus into the rostral spinal cord especially along the central canal. Interestingly, small fibers were not observed in any part of the medulla.

Ventral myelencephalon—In the ventral medulla, medium-sized AVP-ir fibers are found mostly at the midline in the raphe magnus (RMg) and, caudally, the raphe pallidus (RPa; Fig. 20E,F,H). Some medium-sized fibers are seen in a dorsal–ventral orientation passing into the raphe interpositus and, more caudally, the raphe obscurus; this is especially clear in sagittal sections. At the caudal level in which the facial nerve travels dorsally, fibers spread out from the midline into the alpha part of the gigantocellular region. The fibers rarely stray into the larger gigantocellular region and do not extend past the facial nucleus. Sparse to scattered fibers are also observed in the intermediate reticular formation where the facial nerve stretches dorsally. Finally, medium-sized fibers are observed in the lateral reticular formation (LRt; Fig. 20I) and the caudal part of the spinal trigeminal nucleus (Sp5C; Fig. 20J). The innervation of the Sp5C is best observed in sagittal sections, and these fibers may travel into the spinal cord.

Fibers in the spinal cord

The spinal cord contains multiple regions of innervation. Throughout the spinal cord sparse to scattered medium-sized fibers are observed in the dorsal horn (Fig. 21A,–C,F–H). This innervation becomes scattered to moderate in the lumbar cord (Fig. 21G). Fibers appear to be restricted to layers 1 and 2 but may also spread out into layer 3 of the dorsal horn (Fig. 21B). Sagittal sections of the cord suggest that these fibers may be travelling from rostral to caudal through the dorsal horn.

A second pathway, revealed in sagittal sections, is found along and around the central canal in layer 10. Coronal sections show that, along the rostral to caudal extent of the cord, these fibers vary in density more than those found in layers 1 and 2. These fibers are less dense in the cervical (C), caudal thoracic (T), and rostral lumbar (L) cord (Fig. 21A,F,G) but are moderate in density in the rostral thoracic (Fig. 21C,D) and caudal lumbar-sacral (S) cord (Fig. 21H,J). In particular, a moderately dense fiber plexus is located in layer 10 from C8 to T4 rostrally (Fig. 21D) and from L6 to S2 caudally, at which point it spreads dorsally into the sacral dorsal commissural nucleus (Fig. 21J).

In addition, significant lateral projections are observed in the rostral thoracic and sacral cord. Between C8 and T4, the density of fibers around the central canal increases, and, in coronal sections, fibers can be seen projecting laterally toward a dense cluster of fibers located in the intermediolateral column (IML; Fig. 21C,E). The cluster of fibers in the IML is most dense between T1 and T2. A second lateral projection is observed from L6 to S3. In this region, fibers increase in density around the central canal, and fibers can be seen projecting laterally toward a scattered to moderate density of fibers in the sacral parasympathetic nucleus (Fig. 21H,I).

DISCUSSION

The data presented above include the first comprehensive description of AVP-ir fiber distribution in the midbrain, hindbrain, and spinal cord of the mouse. In addition, our data agree with descriptions of AVP-ir fiber location in the telencephalon and diencephalon by Castel and Morris (1988) and Abrahamson et al. (2001) and provide detailed anatomical descriptions regarding major forebrain AVP-ir projection sites not found in any other source. In all, the mouse brain contains one of the densest AVP-ir innervation patterns observed in any species to date. The location of AVP-ir cells in the PVN, SON, SCN, MeA, BNST, and accessory nuclei was similar to previous reports (Castel and Morris, 1988; Abrahamson and Moore, 2001; Ho et al., 2010). No AVP-ir cells were found in other areas, so these cells are presumably the origin for AVP-ir projections throughout the brain, including several areas that have not previously been described from mice such as the ventral tegmental area, interfascicular nucleus, dorsal raphe nucleus, and median raphe, among others. Our data indicate numerous brain areas where AVP can influence the many functions in which it has been implicated, from autonomic function, to circadian rhythms, to learning and memory and social behavior (Goodson and Bass, 2001; Aguilera et al., 2008; Carter et al., 2008; Engelmann, 2008; Veenema and Neumann, 2008; Li et al., 2009).

Experimental considerations

Antibody specificity and sensitivity—Several observations confirm the specificity of our staining. Preadsorption of our antiserum with AVP completely eliminated AVP immunoreactivity. Preadsorption with oxytocin on the other hand did not block staining in any region. This control is important, insofar as oxytocin and AVP differ in only two amino acids, making cross-sensitivity of the antiserum a potential concern. Furthermore, oxytocin-ir cell bodies have never been described in the BNST, MeA, or SCN, which all were shown to contain AVP-ir cell bodies in our study and in numerous others (for review see de Vries and Panzica, 2006). This argument is more difficult to make for AVP-ir cells in the PVN, SON, and accessory nuclei, where the distribution of AVP and oxytocin cells overlaps (Castel and Morris, 1988). However, we did not detect any AVP-ir cells in areas where only oxytocin cells are found, such as the rostral anterior commissural nucleus (De Vries et al., 1985; Castel and Morris, 1988; Abrahamson and Moore, 2001; Rood et al., 2008). Finally, as described in more detail below, AVP-ir projections were present in the mouse that are not found in other species. It is important to note that multiple factors could render our staining more sensitive compared with other studies. In particular, we used acrolein as a fixative instead of paraformaldehyde, which is used in most other studies, and we incubated sections in sodium citrate in an “antigen retrieval” step (Jiao et al., 1999).

Fiber characteristics—The locations of punctate AVP-ir staining associated with small fibers and what appears to be discrete terminal boutons associated with medium-sized fibers suggest numerous sites where AVP could affect physiological or behavioral processes. However, synapses containing AVP immunoreactivity have been observed only in the lateral septum of the rat (Buijs and Swaab, 1979) and SCN (Castel et al., 1990). Thus the

“terminal fields” and “terminal boutons,” associated with small and medium-sized fibers, respectively, can only be considered putative release sites at present. In addition, it is important to note that none of the fiber descriptions to date, including those provided in here, can make accurate claims about whether the immunoreactive fibers observed are dendrites or axons. This is especially important given recent evidence that dendrites, particularly of neurons of the PVN and SON, can release AVP as well (Pow and Morris, 1989; Ludwig and Landgraf, 1992). This not only extends the zone of influence of AVP but suggests that there may be multiple functions and sites of action for a single neuron let alone the numerous cell groups and projection sites found throughout the brain.

We observed, as have others (Castel and Morris, 1988; Abrahamson and Moore, 2001), distinct fiber types, which we called *small*, *medium-sized*, and *large* fibers. These different fiber types are often located in discrete regions (i.e., either small fibers or medium-sized fibers), although we observed many areas of overlap as well. These differences in fiber morphology may reflect differences in the site of origin of the fibers (Abrahamson and Moore, 2001). However, it is impossible to trace these fibers back to their origin using only immunohistochemistry. Currently, the anatomy of AVP projections has been most extensively studied in rats using a variety of methods. For example, lesions of the SCN eliminate small fibers in the dorsomedial hypothalamus, subparaventricular zone, and paraventricular thalamus (Hoorneman and Buijs, 1982); lesions of the BNST eliminate small fibers in the lateral septum and lateral habenula (De Vries and Buijs, 1983); lesions of the medial amygdala eliminate small fibers in the ventral hippocampus (Caffe et al., 1987); and lesions of the PVN eliminate medium-sized fibers in the solitary nucleus (De Vries and Buijs, 1983). In addition, retrograde tracers injected into the ventral hippocampus stain cells in the medial amygdala (Caffe et al., 1987); tracers injected into the brainstem stain cells in the PVN (Sawchenko and Swanson, 1982); and tracers injected in the lateral septum stain the BNST and MeA (De Vries and Buijs, 1983; Caffe et al., 1987). Finally, castration, which eliminates AVP mRNA expression specifically in the BNST and MeA, eliminates immunoreactivity in a subset of fibers, including those found in the lateral septum and lateral habenula (De Vries et al., 1984, 1985). These studies strengthen the assumption that differences in fiber type are related to different origins and delineate the site of origin of AVP-ir fibers in several areas of the rat brain; however, these connections remain to be examined in detail in the mouse. The site of origin of the dense and complex patterns of innervation by small and medium-sized fibers observed in the preoptic area, hypothalamus, and BNST presents a particularly challenging puzzle, and many fibers in the midbrain and hindbrain such as those in the various raphe nuclei, interfascicular nucleus, and ventral tegmental area are of unknown origin.

Species comparisons

In general, the pattern of AVP immunoreactivity in the mouse brain is quite similar to that in other species (for review see Goodson and Bass, 2001), although it is remarkably more robust than has been found in some areas. For example, innervation of the peduncular lateral hypothalamus is much more pronounced than that reported for rats (De Vries et al., 1985). There are other differences between rats and mice. For example, the rat has AVP fibers and cells in the olfactory bulbs and olfactory tubercle (De Vries et al., 1985; Tobin et al., 2010), whereas mice do not. Conversely, AVP fibers are found in the nucleus accumbens and central amygdala of the mouse but are absent or sparse in the rat (De Vries et al., 1985).

Despite numerous similarities across species, there are also a number of species-specific characteristics. For example, AVP-ir fibers are found in auditory nuclei such as the dorsal cochlear nucleus and periolivary region of the guinea pig (Dubois-Dauphin et al., 1989); laterodorsal tegmental nuclei and vestibular nuclei of the jerboa, a desert dwelling rodent

(Lakhdar-Ghazal et al., 1995); and the facial nucleus, pontine nuclei, and lateral geniculate nucleus of the Brazilian opossum (Iqbal and Jacobson, 1995). None of these regions appears to contain AVP immunoreactivity in the mouse. Because these species do not have AVP-ir cells in areas different from mice, it is unclear whether this species difference involves radical differences in projections of AVP-ir cells between mice and these species or whether other factors play a role. The opposite situation is found as well. For example, golden hamsters do not produce AVP in the BNST or MeA, and, as a consequence, all regions that might be innervated by those nuclei, such as the lateral septum and lateral habenula, do not have AVP-ir fibers (Dubois-Dauphin et al., 1990; Albers et al., 1991; Ferris et al., 1995; Miller et al., 1999). Another species, the naked mole rat, appears to lack AVP production in the BNST, MeA, and SCN (Rosen et al., 2007). As a consequence, additional areas such as the subparaventricular zone and dorsomedial hypothalamus have reduced fibers compared with mice. Finally, rats also have AVP-ir cells in the dorsomedial hypothalamus, vertical diagonal band of Broca, and olfactory bulb (Caffe and van Leeuwen, 1983; Planas et al., 1995; Tobin et al., 2010), whereas mice do not. Given the influence of AVP on social behavior (Goodson and Bass, 2001; Carter et al., 2008; Veenema and Neumann, 2008), such species differences in AVP innervation may contribute to species difference in social behavior.

One final observation that bears mention is the remarkable similarity in location of medium-sized AVP-ir fibers as described here and by Castel and Morris (1988) to the location of oxytocin-ir fibers described in mice and rats (Buijs, 1978; Buijs et al., 1978; Swanson and McKellar, 1979; Castel and Morris, 1988). In fact, Castel and Morris (1988), who examined neurophysin-1 (oxytocin-associated) and neurophysin-2 (AVP-associated) immunoreactivity in the forebrain, reported seeing both types of fibers in many of the same areas, including the nucleus accumbens shell, median preoptic area, ventral BNST, central amygdala, and numerous regions of the hypothalamus. The spinal cord provides a particularly poignant cross-species comparison. In mice, AVP-ir fibers are found running along the central canal and in layers 1 and 2 of the gray matter. There are substantial increases in fiber density at certain regions of the thoracic and lumbar-sacral regions where fibers enter the intermediolateral column and sacral parasympathetic nucleus, respectively. Similar projections patterns are observed in the rat when stained for oxytocin or neurophysin-1 (Swanson and McKellar, 1979). The striking similarity in projection sites suggests that these two neuropeptides may interact in these areas.

Novel observations

The discrete localization of fibers in our study reveals a number of novel sites with AVP innervation in the telencephalon and diencephalon. For example, AVP-ir fibers are found in the rostral part of the ventral pallidum, where they spread caudally into the substantia innominata and lateral preoptic area. This network of fibers is less dense than the networks found by us and described by Castel and Morris (1988) in the lateral septum and the area surrounding the diagonal band of Broca. In addition, we observed small-caliber fibers in large but discrete regions of the anterior hypothalamus and lateral hypothalamus, especially rostrally and caudally to the dense projections that appear to exit the PVN. Previously unreported AVP-ir fibers were also observed in several distinct regions of the cerebral cortex, including the cingulate, frontal, and entorhinal cortices. Finally, our data suggest that the BNST contains, aside from AVP-producing cells, a complex region-specific innervation. In particular, its anteromedial and posterior divisions contain variable densities of small fibers, whereas a notable collection of medium-sized fibers occurs in the ventromedial BNST, suggesting multimodal AVP innervation of this area.

Along with previously undocumented fiber projections in the forebrain, our data refine descriptions of fibers in various regions. For example, sagittal and coronal sections suggest

two distinct pathways of fibers ascending along the rostral and dorsal surface of the thalamus, one at the midline and the second more laterally located. The midline pathway appears to be similar to Castel and Morris' description of SCN projections, whereas the lateral projection appears to reach the mediodorsal thalamus, referred to as the *paratenial thalamus* by Castel and Morris (1988), and the lateral habenula, which are both thought to be innervated by the BNST or medial amygdala and not the SCN (De Vries and Buijs, 1983; Rood et al., 2008).

Finally, in addition to the important distinctions made regarding forebrain AVP immunoreactivity, we have examined the midbrain, hindbrain, and spinal cord. These areas contain discrete regions of small fiber innervation within several important regulatory regions of the midbrain, including the ventral tegmental area and dorsal and median raphe nuclei, as well as medium-sized fiber innervation of a number of midbrain, hindbrain, and spinal cord sites associated with autonomic functions.

Functional relevance

Many regions with related functions seemed to be innervated by distinct AVP-ir pathways. For example, medium-sized fibers were observed passing through the periaqueductal gray into the lateral parabrachial nucleus and the solitary nucleus. Some fibers in this pathway appeared to continue caudally at the midline along the fourth ventricle and central canal. Sagittal sections near the midline indeed showed fibers travelling rostral to caudal in the hindbrain (see Fig. 20F); similarly oriented fibers were observed in spinal cord sections as well. Robust increases in fiber density along this pathway were observed in the solitary nucleus in the hindbrain and the intermediolateral nucleus (IML) and sacral parasympathetic nucleus (SPSy) in the spinal cord. The IML and SPSy contain neurons that are part of the sympathetic and parasympathetic nervous systems, respectively (Kuo et al., 1984; Chung et al., 1993). The solitary nucleus acts as a sensory relay for information from a number of peripheral organ systems and appears to be important in the control or regulation of cardiovascular, respiratory, and gastrointestinal reflexes (Andresen and Kunze, 1994). The lateral parabrachial nucleus is thought to be involved in the behavioral regulation of water balance and salt intake and receives projections from the solitary nucleus (Menani et al., 1996). These regions all appear to be involved in the regulation of autonomic sensory information and behavioral responses to autonomic information. Of particular interest is the role of these areas in controlling cardiovascular function, water balance, and salt intake given the well-known peripheral action of AVP on these functions. The central nervous system AVP projections along this rostral to caudal medium-sized fiber pathway may therefore be positioned to provide neural regulation in line with peripheral AVP release. These pathways also suggest an important role in control of the sympathetic and parasympathetic nervous system, as has been suggested for rats (Sawchenko and Swanson, 1982).

A second example of a functional pathway is the small AVP-ir fibers that become prominent near the caudal part of the lateral hypothalamus at the level of the mammillary bodies. At least some of these fibers appear to continue into the ventral tegmental area (VTA), then through the caudal linear raphe, and finally into the dorsal raphe. Although this pathway can only be loosely inferred from the coronal view, sagittal sections more clearly illustrate fibers following the trajectory outlined above. Punctate terminal fields were most prominent in the VTA and interfascicular nuclei, which are the primary producers of dopamine in the mesolimbic dopamine system (Nelson et al., 1996), and the median and dorsal raphe, which are the primary producers of serotonin for forebrain projections (Steinbusch, 1981). Furthermore, the mesolimbic dopamine system has been implicated in motivation and reward and the serotonin system in anxiety and depression (Spanagel and Weiss, 1999;

Michelsen et al., 2007). Thus our anatomical data suggest that AVP could potentially affect major regulatory systems involved in controlling behavioral and emotional state.

These findings are even more salient given that AVP has been implicated in the regulation of social behavior, which is likely influenced by an animal's emotional state. What is more, several other brain regions specifically implicated in social behavior contained AVP-ir fibers. The most prominent examples are the medial amygdala, lateral septum, and medial preoptic area. The medial amygdala, which contains a dense innervation of small AVP-ir fibers, receives information from and sends information to the accessory olfactory system (Martel and Baum, 2009). The accessory olfactory system is thought to provide social information carried by pheromones (Keller et al., 2009). The lateral septum is perhaps the most well-studied brain region in terms of AVP and social behavior. AVP in this region is thought to facilitate social memory. AVP agonists injected into the lateral septum facilitate the memory of a same-sex conspecific, but AVP antagonists disrupt this social memory (Dantzer et al., 1987, 1988). Our findings of AVP in regulatory regions in conjunction with other observed fiber projection sites suggest that AVP may be part of a larger system that integrates sensory information and prepares an animal to respond appropriately to a given social situation by altering memory function, motivation, arousal, and emotional state.

The AVP innervation of various midline and lateral nuclei of the diencephalon suggests yet other functions that may be influenced by AVP. In the hypothalamus, medial regions containing small, punctate AVP-ir staining include the anteroventral periventricular area and periventricular zone, which are areas important for neuroendocrine control (Markakis, 2002), and the subparaventricular zone and dorsomedial hypothalamus, which in the rat are well known sites of SCN innervation and are thought to be involved in regulation of behavioral circadian rhythms (Chou et al., 2003; Li et al., 2009). In fact, AVP projections from the SCN to these areas have recently been implicated in the control of circadian rhythms in the hypothalamic–pituitary–adrenal and hypothalamic–pituitary–gonadal axes (Kalsbeek et al., 2010). Lateral regions of innervation by small AVP-ir fibers are found in the lateral preoptic area and lateral hypothalamus. These areas are generally thought to be involved in the regulation of behavior, although there appear to be few well-delineated functions with the exception of the role of the lateral hypothalamus in food intake and reward, especially in the context of the orexin system (Kotz, 2006). In the thalamus, the midline nuclei, including the paraventricular nuclei, are thought to be involved in awareness processing and may be specific to visceral and limbic information (Van der Werf et al., 2002). In contrast, the mediodorsal nucleus, which flanks the PV laterally, is thought to be involved in cognitive awareness. Furthermore, the mediodorsal thalamus is the thalamic component of a basal ganglia circuit regulating activity of the prefrontal cortex, which is involved in cognition (Chauveau et al., 2005; Mitchell et al., 2007; Mitchell and Gaffan, 2008). The more caudal lateral habenula serves as a relay for hypothalamic information to regulatory nuclei such as the VTA and dorsal raphe (Wang and Aghajanian, 1977; Hikosaka et al., 2008), which, as discussed above, contain small AVP-ir fibers as well.

Work in rats suggests that the midline and medial regions discussed here receive their AVP innervation from the SCN (Hoorneman and Buijs, 1982; Abrahamson and Moore, 2001), whereas lateral regions receive their AVP innervation from the BNST or MeA (De Vries and Buijs, 1983; Caffé et al., 1987). This remains to be shown in the mouse but nevertheless has important implications regarding the function of AVP in the various diencephalic nuclei. If true, then the AVP-ir fibers from the SCN would be well positioned to affect neuroendocrine systems and arousal and awareness systems, which are functions with distinct circadian patterns (Chou et al., 2003). In contrast, the lateral regions, if innervated by BNST or medial amygdala AVP neurons, could affect cognitive and behavioral outcomes

in social situations, a leading hypothesis for the function of AVP originating in the BNST and medial amygdala (Caldwell et al., 2008; Ho et al., 2010).

CONCLUSIONS

The results of our study illustrate a complicated network of AVP-ir innervation throughout the brain and spinal cord of the mouse. Our findings confirm and expand our understanding of AVP-ir fiber location in the forebrain and provide new information on projections to the midbrain, hindbrain, and spinal cord of the mouse. Despite the large number of projections sites, several functional systems are apparent. Medium-sized AVP fibers innervate a number of nuclei involved in autonomic functions such as water balance and blood pressure regulation (e.g., the lateral parabrachial nucleus and solitary nucleus in the brain and the intermediolateral nucleus and sacral parasympathetic nucleus in the spinal cord). In addition to the well-studied AVP projections from the BNST and medial amygdala projections to the lateral septum, other projections may be of particular interest in the study social behavior. For example, the dorsal and median raphe nuclei and the lateral habenular nucleus contain small fibers. The raphe nuclei contain serotonergic cells that have broad projections throughout the brain and are critical for the control of emotional state (Cools et al., 2008), whereas the lateral habenula is part of a modulatory loop referred to as the *dorsal diencephalic conduction system* and is thought to integrate hypothalamic input and alter neuronal activity in the dorsal raphe and ventral tegmental area (Reisine et al., 1982; Sutherland, 1982; Hikosaka et al., 2008). AVP-ir fibers are also found in the ventral tegmental area, interfascicular nucleus, ventral pallidum, and mediodorsal thalamus. These nuclei are all part of basal ganglia loops often referred to as the limbic loop and cortical loop of the basal ganglia, which mirror motor loops involved in disorders such as Parkinson's and Huntington's diseases. These two neural systems in particular have been implicated in numerous emotional and behavioral disorders such as anxiety, depression, and schizophrenia (Nestler and Carlezon, 2006; Alelu-Paz and Gimenez-Amaya, 2008; Hikosaka et al., 2008). Polymorphisms in the AVP V1a receptor gene have been linked to disorders including schizophrenia, depression, and autism (Kim et al., 2002; van West et al., 2004; Levin et al., 2009). Ultimately, understanding the functional role of AVP in brain regions identified here and elsewhere may very well help us to elucidate and understand neural circuits critically involved in some of the most socially and economically costly behavioral disorders.

Acknowledgments

Grant sponsor: National Science Foundation; Grant number: IBN 9421658; Grant sponsor: National Institute of Mental Health; Grant number: RO1 MH047538; Grant number: T32 MH020051.

Abbreviations

2Cb	lobule 2 of the cerebellar vermis
3n	oculomotor nerve
3V	3rd ventricle
4n	trochlear nerve
4N	trochlear nucleus
7n	facial nerve
12N	hypoglossal nucleus
AA	anterior amygdaloid area

ac	anterior commissure
AcbC	accumbens nucleus, core
AcbSh	accumbens nucleus, shell
ACo	anterior cortical amygdaloid area
AH	anterior hypothalamus
AHA	anterior hypothalamic area, anterior part
AHC	anterior hypothalamic area, central part
AHiPM	amygdalohippocampal area, posteromedial part
Aq	aqueduct
Arc	arcuate hypothalamic nucleus
ATg	anterior tegmental nucleus
AVPe	anteroventral periventricular nucleus
bas	basilar artery
BLP	basolateral amygdaloid n., posterior part
BMA	basomedial amygdaloid n., anterior part
BNST	bed nucleus of the stria terminalis
cc	corpus callosum
BSTLV	BNST, lateral division, ventral
BSTMA	BNST, medial division, anterior
BSTMPI	BNST, medial division, posterior intermediate
BSTMPL	BNST, medial division, posterolateral
BSTMPM	BNST, medial division, posteromedial
BSTMV	BNST, medial division, ventral part
CeA	central amygdala
Cg2	cingulate cortex, area 2
Cl	claustrum
CLi	caudal linear nucleus of the raphe
CM	central medial thalamic nucleus
cp	cerebral peduncle
CPu	caudate putamen (striatum)
csc	commissure of the superior colliculus
CxA	cortex–amygdala transition zone
D3V	dorsal 3rd ventricle
DLEnt	dorsolateral entorhinal cortex
DM	dorsomedial hypothalamic nucleus
DMPAG	dorsomedial periaqueductal gray

DR	dorsal raphe nucleus
DRC	dorsal raphe nucleus, caudal part
DRD	dorsal raphe nucleus, dorsal part
DRL	dorsal raphe nucleus, lateral part
DTM	dorsal tuberomammillary nucleus
EA	extended amygdala
f	fornix
fr	fasciculus retroflexus
Gi	gigantocellular reticular nucleus
GiA	gigantocellular reticular n., alpha part
GP	globus pallidus
Gr	gracile nucleus
hbc	habenular commissure
HDB	horizontal limb of the diagonal band
IAD	interanterodorsal thalamic nucleus
ic	internal capsule
ICjM	island of Calleja, major island
IF	interfascicular nucleus
IMD	intermediodorsal thalamic nucleus
IO	inferior olivary nucleus
IP	interpeduncular nucleus
IPR	interpeduncular n., rostral subnucleus
IRt	intermediate reticular nucleus
LA	lateroanterior hypothalamic nucleus
La	lateral amygdaloid nucleus
LC	locus coeruleus
LDTg	laterodorsal tegmental nucleus
LHb	lateral habenular nucleus
LMol	lacunosum moleculare layer of the hippocampus
LOT	nucleus of the lateral olfactory tract
LPB	lateral parabrachial nucleus
LPO	lateral preoptic area
LRt	lateral reticular nucleus
LS	lateral septum
ll	lateral lemniscus
LSD	lateral septal nucleus, dorsal part

LSI	lateral septal nucleus, intermediate part
LSO	lateral superior olive
LSV	lateral septal nucleus, ventral part
LV	lateral ventricle
MB	mammillary bodies
MD	mediodorsal thalamic nucleus
ME	median eminence
MeA	medial amygdaloid nucleus, anterior part
MePD	medial amygdaloid n., posterodorsal part
ml	medial lemniscus
mlf	medial longitudinal fasciculus
MnPO	median preoptic nucleus
MnR	median raphe nucleus
MPA	medial preoptic area
MPB	medial parabrachial nucleus
MPOM	medial preoptic nucleus, medial part
MRe	mammillary recess of the 3rd ventricle
MS	medial septal nucleus
mt	mammillothalamic tract
MTeg	midbrain tegmentum
ROb	raphe obscurus nucleus
RPa	raphe pallidus nucleus
RRF	retrochiasmatic field
SCN	suprachiasmatic nucleus
scp	superior cerebellar peduncle
SFi	septo-fimbrial nucleus
SFO	subfornical organ
SHy	septo-hypothalamic nucleus
SI	substantia innominata
SM	nucleus of the stria medullaris
sm	stria medullaris
SNR	substantia nigra, reticular part
SON	supraoptic nucleus
SOR	supraoptic nucleus, retrochiasmatic part
sp5	spinal trigeminal tract
Sp5C	spinal trigeminal nucleus, caudal part

SPa	subparaventricular zone
SPO	superior paraolivary nucleus
st	stria terminalis
StHy	striohypothalamic nucleus
SubB	subbrachial nucleus
ts	tectospinal tract
Tu	olfactory tubercle
TuLH	tuberal region of lateral hypothalamus
VDB	vertical limb of the diagonal band
VLPA	ventrolateral periaqueductal gray
VLPO	ventrolateral preoptic nucleus
VMH	ventromedial hypothalamic nucleus
VMPO	ventromedial preoptic nucleus
VOLT	vascular organ of the lamina terminalis
VP	ventral pallidum
VS	ventral subiculum
VSA	ventral septal area
vsc	ventral spinocerebellar tract
VTA	ventral tegmental area
vtgx	ventral tegmental decussation
VTM	ventral tuberomammillary nucleus
Xi	xiphoid thalamic nucleus
xscp	decussation of the superior cerebellar peduncle
ZI	zona incerta

LITERATURE CITED

- Abrahamson EE, Moore RY. Suprachiasmatic nucleus in the mouse: retinal innervation, intrinsic organization and efferent projections. *Brain Res.* 2001; 916:172–191. [PubMed: 11597605]
- Aguilera G, Subburaju S, Young S, Chen J. The parvo-cellular vasopressinergic system and responsiveness of the hypothalamic pituitary adrenal axis during chronic stress. *Prog Brain Res.* 2008; 170:29–39. [PubMed: 18655869]
- Albers HE, Rowland CM, Ferris CF. Arginine-vasopressin immunoreactivity is not altered by photoperiod or gonadal hormones in the Syrian hamster (*Mesocricetus auratus*). *Brain Res.* 1991; 539:137–142. [PubMed: 2015498]
- Alelu-Paz R, Gimenez-Amaya JM. The mediodorsal thalamic nucleus and schizophrenia. *J Psychiatry Neurosci.* 2008; 33:489–498. [PubMed: 18982171]
- Andresen MC, Kunze DL. Nucleus tractus solitarius—gateway to neural circulatory control. *Annu Rev Physiol.* 1994; 56:93–116. [PubMed: 7912060]
- Bamshad M, Novak MA, De Vries GJ. Sex and species differences in the vasopressin innervation of sexually naive and parental prairie voles, *Microtus ochrogaster*, and meadow voles, *Microtus pennsylvanicus*. *J Neuroendocrinol.* 1993; 5:247–255. [PubMed: 8319000]

- Banet M, Wieland UE. The effect of intraseptally applied vasopressin on thermoregulation in the rat. *Brain Res Bull.* 1985; 14:113–116. [PubMed: 3995357]
- Bester-Meredith JK, Young LJ, Marler CA. Species differences in paternal behavior and aggression in *Peromyscus* and their associations with vasopressin immunoreactivity and receptors. *Horm Behav.* 1999; 36:25–38. [PubMed: 10433884]
- Bielsky IF, Hu SB, Szegda KL, Westphal H, Young LJ. Profound impairment in social recognition and reduction in anxiety-like behavior in vasopressin V1a receptor knockout mice. *Neuropsychopharmacology.* 2004; 29:483–493. [PubMed: 14647484]
- Buijs RM, Swaab DF. Immuno-electron microscopical demonstration of vasopressin and oxytocin synapses in the limbic system of the rat. *Cell Tissue Res.* 1979; 204:355–365. [PubMed: 527026]
- Buijs RM. Intra- and extrahypothalamic vasopressin and oxytocin pathways in the rat. Pathways to the limbic system, medulla oblongata and spinal cord. *Cell Tissue Res.* 1978; 192:423–435. [PubMed: 699026]
- Buijs RM, Swaab DF, Dogterom J, van Leeuwen FW. Intra- and extrahypothalamic vasopressin and oxytocin pathways in the rat. *Cell Tissue Res.* 1978; 186:423–433. [PubMed: 342106]
- Caffe AR, van Leeuwen FW. Vasopressin-immunoreactive cells in the dorsomedial hypothalamic region, medial amygdaloid nucleus and locus coeruleus of the rat. *Cell Tissue Res.* 1983; 233:23–33. [PubMed: 6616564]
- Caffe AR, van Leeuwen FW, Luiten PG. Vasopressin cells in the medial amygdala of the rat project to the lateral septum and ventral hippocampus. *J Comp Neurol.* 1987; 261:237–252. [PubMed: 3305600]
- Caffe AR, Van Ryen PC, Van der Woude TP, Van Leeuwen FW. Vasopressin and oxytocin systems in the brain and upper spinal cord of *Macaca fascicularis*. *J Comp Neurol.* 1989; 287:302–325. [PubMed: 2778107]
- Caldwell HK, Lee HJ, Macbeth AH, Young WS 3rd. Vasopressin: behavioral roles of an “original” neuropeptide. *Prog Neurobiol.* 2008; 84:1–24. [PubMed: 18053631]
- Carter CS, Grippo AJ, Pournajafi-Nazarloo H, Ruscio MG, Porges SW. Oxytocin, vasopressin and sociality. *Prog Brain Res.* 2008; 170:331–336. [PubMed: 18655893]
- Castel M, Morris JF. The neurophysin-containing innervation of the forebrain of the mouse. *Neuroscience.* 1988; 24:937–966. [PubMed: 3380308]
- Castel M, Feinstein N, Cohen S, Harari N. Vasopressinergic innervation of the mouse suprachiasmatic nucleus: an immuno-electron microscopic analysis. *J Comp Neurol.* 1990; 298:172–187. [PubMed: 2212101]
- Chauveau F, Celerier A, Ognard R, Pierard C, Beracochea D. Effects of ibotenic acid lesions of the mediodorsal thalamus on memory: relationship with emotional processes in mice. *Behav Brain Res.* 2005; 156:215–223. [PubMed: 15582107]
- Chou TC, Scammell TE, Gooley JJ, Gaus SE, Saper CB, Lu J. Critical role of dorsomedial hypothalamic nucleus in a wide range of behavioral circadian rhythms. *J Neurosci.* 2003; 23:10691–10702. [PubMed: 14627654]
- Chung K, Lee WT, Park MJ. Spinal projections of pelvic visceral afferents of the rat: a calcitonin gene-related peptide (CGRP) immunohistochemical study. *J Comp Neurol.* 1993; 337:63–69. [PubMed: 8276992]
- Compaan JC, Buijs RM, Pool CW, De Ruiter AJ, Koolhaas JM. Differential lateral septal vasopressin innervation in aggressive and nonaggressive male mice. *Brain Res Bull.* 1993; 30:1–6. [PubMed: 8420617]
- Cools R, Roberts AC, Robbins TW. Serotonergic regulation of emotional and behavioural control processes. *Trends Cogn Sci.* 2008; 12:31–40. [PubMed: 18069045]
- Dantzer R, Bluthé RM, Koob GF, Le Moal M. Modulation of social memory in male rats by neurohypophyseal peptides. *Psychopharmacology.* 1987; 91:363–368. [PubMed: 3104959]
- Dantzer R, Koob GF, Bluthé RM, Le Moal M. Septal vasopressin modulates social memory in male rats. *Brain Res.* 1988; 457:143–147. [PubMed: 3167559]
- De Vries GJ, Buijs RM. The origin of the vasopressinergic and oxytocinergic innervation of the rat brain with special reference to the lateral septum. *Brain Res.* 1983; 273:307–317. [PubMed: 6311351]

- De Vries GJ, Panzica GC. Sexual differentiation of central vasopressin and vasotocin systems in vertebrates: different mechanisms, similar endpoints. *Neuroscience*. 2006; 138:947–955. [PubMed: 16310321]
- De Vries GJ, Buijs RM, Sluiter AA. Gonadal hormone actions on the morphology of the vasopressinergic innervation of the adult rat brain. *Brain Res*. 1984; 298:141–145. [PubMed: 6722551]
- De Vries GJ, Buijs RM, Van Leeuwen FW, Caffé AR, Swaab DF. The vasopressinergic innervation of the brain in normal and castrated rats. *J Comp Neurol*. 1985; 233:236–254. [PubMed: 3882778]
- Demotes-Mainard J, Chauveau J, Rodriguez F, Vincent JD, Pou-lain DA. Septal release of vasopressin in response to osmotic, hypovolemic and electrical stimulation in rats. *Brain Res*. 1986; 381:314–321. [PubMed: 3756507]
- Dubois-Dauphin M, Tribollet E, Dreifuss JJ. Distribution of neurohypophysial peptides in the guinea pig brain. I. An immunocytochemical study of the vasopressin-related glycopeptide. *Brain Res*. 1989; 496:45–65. [PubMed: 2804653]
- Dubois-Dauphin M, Pevet P, Tribollet E, Dreifuss JJ. Vasopressin in the brain of the golden hamster: the distribution of vasopressin binding sites and of immunoreactivity to the vasopressin-related glycopeptide. *J Comp Neurol*. 1990; 300:535–548. [PubMed: 2148751]
- Engelmann M. Vasopressin in the septum: not important versus causally involved in learning and memory—two faces of the same coin? *Prog Brain Res*. 2008; 170:389–395. [PubMed: 18655898]
- Farini F. Diabete insipido ed opoteria. *Gazz Osped Clin*. 1913; 34
- Ferris CF, Albers HE, Wesolowski SM, Goldman BD, Luman SE. Vasopressin injected into the hypothalamus triggers a stereotypic behavior in golden hamsters. *Science*. 1984; 224:521–523. [PubMed: 6538700]
- Ferris CF, Meenan DM, Albers HE. Microinjection of kainic acid into the hypothalamus of golden hamsters prevents vasopressin-dependent flank-marking behavior. *Neuroendocrinology*. 1986; 44:112–116. [PubMed: 3785573]
- Ferris CF, Delville Y, Miller MA, Dorsa DM, De Vries GJ. Distribution of small vasopressinergic neurons in golden hamsters. *J Comp Neurol*. 1995; 360:589–598. [PubMed: 8801251]
- Franklin, KBJ.; Paxinos, G. *The mouse brain in stereotaxic coordinates*. Elsevier; Amsterdam: 2008.
- Goodson JL, Bass AH. Social behavior functions and related anatomical characteristics of vasotocin/vasopressin systems in vertebrates. *Brain Res Brain Res Rev*. 2001; 35:246–265. [PubMed: 11423156]
- Hikosaka O, Sesack SR, Lecourtier L, Shepard PD. Habenula: crossroad between the basal ganglia and the limbic system. *J Neurosci*. 2008; 28:11825–11829. [PubMed: 19005047]
- Ho JM, Murray JH, Demas GE, Goodson JL. Vasopressin cell groups exhibit strongly divergent responses to copulation and male–male interactions in mice. *Horm Behav*. 2010; 58:368–377. [PubMed: 20382147]
- Hoorneman EM, Buijs RM. Vasopressin fiber pathways in the rat brain following suprachiasmatic nucleus lesioning. *Brain Res*. 1982; 243:235–241. [PubMed: 7049323]
- Insel TR, Wang ZX, Ferris CF. Patterns of brain vasopressin receptor distribution associated with social organization in microtine rodents. *J Neurosci*. 1994; 14:5381–5392. [PubMed: 8083743]
- Iqbal J, Jacobson CD. Ontogeny of arginine vasopressin-like immunoreactivity in the Brazilian opossum brain. *Brain Res Dev Brain Res*. 1995; 89:11–32.
- Jiao Y, Sun Z, Lee T, Fusco FR, Kimble TD, Meade CA, Cuthbertson S, Reiner A. A simple and sensitive antigen retrieval method for free-floating and slide-mounted tissue sections. *J Neurosci Methods*. 1999; 93:149–162. [PubMed: 10634500]
- Kalsbeek A, Fliers E, Hofman MA, Swaab DF, Buijs RM. Vasopressin and the output of the hypothalamic biological clock. *J Neuroendocrinol*. 2010; 22:362–372. [PubMed: 20088910]
- Keller M, Baum MJ, Brock O, Brennan PA, Bakker J. The main and the accessory olfactory systems interact in the control of mate recognition and sexual behavior. *Behav Brain Res*. 2009; 200:268–276. [PubMed: 19374011]
- Kim SJ, Young LJ, Gonen D, Veenstra-VanderWeele J, Courchesne R, Courchesne E, Lord C, Leventhal BL, Cook EH Jr, Insel TR. Transmission disequilibrium testing of arginine vasopressin

- receptor 1A (AVPR1A) polymorphisms in autism. *Mol Psychiatry*. 2002; 7:503–507. [PubMed: 12082568]
- Kotz CM. Integration of feeding and spontaneous physical activity: role for orexin. *Physiol Behav*. 2006; 88:294–301. [PubMed: 16787655]
- Krisch B. Immunohistochemical and electron microscopic study of the rat hypothalamic nuclei and cell clusters under various experimental conditions. Possible sites of hormone release. *Cell Tissue Res*. 1976; 174:109–127.
- Kuo DC, Oravitz JJ, DeGroat WC. Tracing of afferent and efferent pathways in the left inferior cardiac nerve of the cat using retrograde and transganglionic transport of horseradish peroxidase. *Brain Res*. 1984; 321:111–118. [PubMed: 6498506]
- Lakhdar-Ghazal N, Dubois-Dauphin M, Hermes ML, Buijs RM, Bengelloun WA, Pevet P. Vasopressin in the brain of a desert hibernator, the jerboa (*Jaculus orientalis*): presence of sexual dimorphism and seasonal variation. *J Comp Neurol*. 1995; 358:499–517. [PubMed: 7593745]
- Landgraf R, Gerstberger R, Montkowski A, Probst JC, Wotjak CT, Holsboer F, Engelmann M. V1 vasopressin receptor antisense oligodeoxynucleotide into septum reduces vasopressin binding, social discrimination abilities, and anxiety-related behavior in rats. *J Neurosci*. 1995; 15:4250–4258. [PubMed: 7790909]
- Landgraf R, Frank E, Aldag JM, Neumann ID, Sharer CA, Ren X, Terwilliger EF, Niwa M, Wigger A, Young LJ. Viral vector-mediated gene transfer of the vole V1a vasopressin receptor in the rat septum: improved social discrimination and active social behaviour. *Eur J Neurosci*. 2003; 18:403–411. [PubMed: 12887422]
- Levin R, Heresco-Levy U, Bachner-Melman R, Israel S, Shalev I, Ebstein R. Association between arginine vasopressin 1a receptor (AVPR1a) promoter region polymorphisms and prepulse inhibition. *Psychoneuroendocrinology*. 2009; 34:901–908. [PubMed: 19195791]
- Li JD, Burton KJ, Zhang C, Hu SB, Zhou QY. Vasopressin receptor V1a regulates circadian rhythms of locomotor activity and expression of clock-controlled genes in the suprachiasmatic nuclei. *Am J Physiol Regul Integr Comp Physiol*. 2009; 296:R824–R830. [PubMed: 19052319]
- Lim MM, Young LJ. Vasopressin-dependent neural circuits underlying pair bond formation in the monogamous prairie vole. *Neuroscience*. 2004; 125:35–45. [PubMed: 15051143]
- Lim MM, Wang Z, Olazabal DE, Ren X, Terwilliger EF, Young LJ. Enhanced partner preference in a promiscuous species by manipulating the expression of a single gene. *Nature*. 2004; 429:754–757. [PubMed: 15201909]
- Ludwig M, Landgraf R. Does the release of vasopressin within the supraoptic nucleus of the rat brain depend upon changes in osmolality and Ca^{2+}/K^{+} ? *Brain Res*. 1992; 576:231–234. [PubMed: 1515919]
- Ludwig M, Leng G. Dendritic peptide release and peptide-dependent behaviours. *Nat Rev Neurosci*. 2006; 7:126–136. [PubMed: 16429122]
- Markakis EA. Development of the neuroendocrine hypothalamus. *Front Neuroendocrinol*. 2002; 23:257–291. [PubMed: 12127306]
- Martel KL, Baum MJ. A centrifugal pathway to the mouse accessory olfactory bulb from the medial amygdala conveys gender-specific volatile pheromonal signals. *Eur J Neurosci*. 2009; 29:368–376. [PubMed: 19077123]
- Menani JV, Thunhorst RL, Johnson AK. Lateral parabrachial nucleus and serotonergic mechanisms in the control of salt appetite in rats. *Am J Physiol*. 1996; 270:R162–R168. [PubMed: 8769798]
- Michelsen KA, Schmitz C, Steinbusch HW. The dorsal raphe nucleus—from silver stainings to a role in depression. *Brain Res Rev*. 2007; 55:329–342. [PubMed: 17316819]
- Miller MA, Ferris CF, Kolb PE. Absence of vasopressin expression by galanin neurons in the golden hamster: implications for species differences in extrahypothalamic vasopressin pathways. *Brain Res Mol Brain Res*. 1999; 67:28–35. [PubMed: 10101229]
- Mitchell AS, Gaffan D. The magnocellular mediodorsal thalamus is necessary for memory acquisition, but not retrieval. *J Neurosci*. 2008; 28:258–263. [PubMed: 18171943]
- Mitchell AS, Browning PG, Baxter MG. Neurotoxic lesions of the medial mediodorsal nucleus of the thalamus disrupt reinforcer devaluation effects in rhesus monkeys. *J Neurosci*. 2007; 27:11289–11295. [PubMed: 17942723]

- Naylor AM, Ruwe WD, Kohut AF, Veale WL. Perfusion of vasopressin within the ventral septum of the rabbit suppresses endotoxin fever. *Brain Res Bull.* 1985; 15:209–213. [PubMed: 3876142]
- Nelson EL, Liang CL, Sinton CM, German DC. Midbrain dopaminergic neurons in the mouse: computer-assisted mapping. *J Comp Neurol.* 1996; 369:361–371. [PubMed: 8743418]
- Nestler EJ, Carlezon WA Jr. The mesolimbic dopamine reward circuit in depression. *Biol Psychiatry.* 2006; 59:1151–1159. [PubMed: 16566899]
- Oliver G, Schafer EA. On the physiological action of extracts of pituitary body and certain other glandular organs: preliminary communication. *J Physiol.* 1895; 18:277–279.
- Ostrowski NL, Lolait SJ, Bradley DJ, O'Carroll AM, Brownstein MJ, Young WS 3rd. Distribution of V1a and V2 vasopressin receptor messenger ribonucleic acids in rat liver, kidney, pituitary and brain. *Endocrinology.* 1992; 131:533–535. [PubMed: 1535312]
- Ostrowski NL, Lolait SJ, Young WS 3rd. Cellular localization of vasopressin V1a receptor messenger ribonucleic acid in adult male rat brain, pineal, and brain vasculature. *Endocrinology.* 1994; 135:1511–1528. [PubMed: 7925112]
- Pitkow LJ, Sharer CA, Ren X, Insel TR, Terwilliger EF, Young LJ. Facilitation of affiliation and pair-bond formation by vasopressin receptor gene transfer into the ventral fore-brain of a monogamous vole. *J Neurosci.* 2001; 21:7392–7396. [PubMed: 11549749]
- Pittman QJ, Franklin LG. Vasopressin antagonist in nucleus tractus solitarius/vagal area reduces pressor and tachycardia responses to paraventricular nucleus stimulation in rats. *Neurosci Lett.* 1985; 56:155–160. [PubMed: 3925390]
- Planas B, Kolb PE, Raskind MA, Miller MA. Vasopressin and galanin mRNAs coexist in the nucleus of the horizontal diagonal band: a novel site of vasopressin gene expression. *J Comp Neurol.* 1995; 361:48–56. [PubMed: 8550881]
- Pow DV, Morris JF. Dendrites of hypothalamic magno-cellular neurons release neurohypophysial peptides by exocytosis. *Neuroscience.* 1989; 32:435–439. [PubMed: 2586758]
- Reisine TD, Soubrie P, Artaud F, Glowinski J. Involvement of lateral habenula-dorsal raphe neurons in the differential regulation of striatal and nigral serotonergic transmission cats. *J Neurosci.* 1982; 2:1062–1071. [PubMed: 6180148]
- Rood BD, Murray EK, Laroche J, Yang MK, Blaustein JD, De Vries GJ. Absence of progesterin receptors alters distribution of vasopressin fibers but not sexual differentiation of vasopressin system in mice. *Neuroscience.* 2008; 154:911–921. [PubMed: 18514427]
- Rosen GJ, De Vries GJ, Goldman SL, Goldman BD, Forger NG. Distribution of vasopressin in the brain of the eusocial naked mole-rat. *J Comp Neurol.* 2007; 500:1093–1105. [PubMed: 17183541]
- Saito M, Sugimoto T, Tahara A, Kawashima H. Molecular cloning and characterization of rat V1b vasopressin receptor: evidence for its expression in extra-pituitary tissues. *Biochem Biophys Res Commun.* 1995; 212:751–757. [PubMed: 7626108]
- Sawchenko PE, Swanson LW. Immunohistochemical identification of neurons in the paraventricular nucleus of the hypothalamus that project to the medulla or to the spinal cord in the rat. *J Comp Neurol.* 1982; 205:260–272. [PubMed: 6122696]
- Spanagel R, Weiss F. The dopamine hypothesis of reward: past and current status. *Trends Neurosci.* 1999; 22:521–527. [PubMed: 10529820]
- Steinbusch HW. Distribution of serotonin-immunoreactivity in the central nervous system of the rat: cell bodies and terminals. *Neuroscience.* 1981; 6:557–618. [PubMed: 7017455]
- Sutherland RJ. The dorsal diencephalic conduction system: a review of the anatomy and functions of the habenular complex. *Neurosci Biobehav Rev.* 1982; 6:1–13. [PubMed: 7041014]
- Swanson LW, McKellar S. The distribution of oxytocin and neurophysin-stained fibers in the spinal cord of the rat and monkey. *J Comp Neurol.* 1979; 188:87–106. [PubMed: 115910]
- Thompson RR, George K, Walton JC, Orr SP, Benson J. Sex-specific influences of vasopressin on human social communication. *Proc Natl Acad Sci U S A.* 2006; 103:7889–7894. [PubMed: 16682649]
- Tobin VA, Hashimoto H, Wacker DW, Takayanagi Y, Langnaese K, Caqueneau C, Noack J, Landgraf R, Onaka T, Leng G, Meddle SL, Engelmann M, Ludwig M. An intrinsic vasopressin system in the olfactory bulb is involved in social recognition. *Nature.* 2010; 464:413–417. [PubMed: 20182426]

- Van der Werf YD, Witter MP, Groenewegen HJ. The intralaminar and midline nuclei of the thalamus. Anatomical and functional evidence for participation in processes of arousal and awareness. *Brain Res Brain Res Rev.* 2002; 39:107–140. [PubMed: 12423763]
- van West D, Del-Favero J, Aulchenko Y, Oswald P, Souery D, Forsgren T, Sluijs S, Bel-Kacem S, Adolfsson R, Mendlewicz J, Van Duijn C, Deboutte D, Van Broeckhoven C, Claes S. A major SNP haplotype of the arginine vasopressin 1B receptor protects against recurrent major depression. *Mol Psychiatry.* 2004; 9:287–292. [PubMed: 15094789]
- Veenema AH, Neumann ID. Central vasopressin and oxytocin release: regulation of complex social behaviours. *Prog Brain Res.* 2008; 170:261–276. [PubMed: 18655888]
- Wang RY, Aghajanian GK. Physiological evidence for habenula as major link between forebrain and midbrain raphe. *Science.* 1977; 197:89–91. [PubMed: 194312]
- Wersinger SR, Ginns EI, O'Carroll AM, Lolait SJ, Young WS 3rd. Vasopressin V1b receptor knockout reduces aggressive behavior in male mice. *Mol Psychiatry.* 2002; 7:975–984. [PubMed: 12399951]
- Yates FE, Russell SM, Dallman MF, Hodge GA, McCann SM, Dhariwal AP. Potentiation by vasopressin of corticotropin release induced by corticotropin-releasing factor. *Endocrinology.* 1971; 88:3–15. [PubMed: 4320769]
- Young LJ, Nilsen R, Waymire KG, MacGregor GR, Insel TR. Increased affiliative response to vasopressin in mice expressing the V1a receptor from a monogamous vole. *Nature.* 1999; 400:766–768. [PubMed: 10466725]

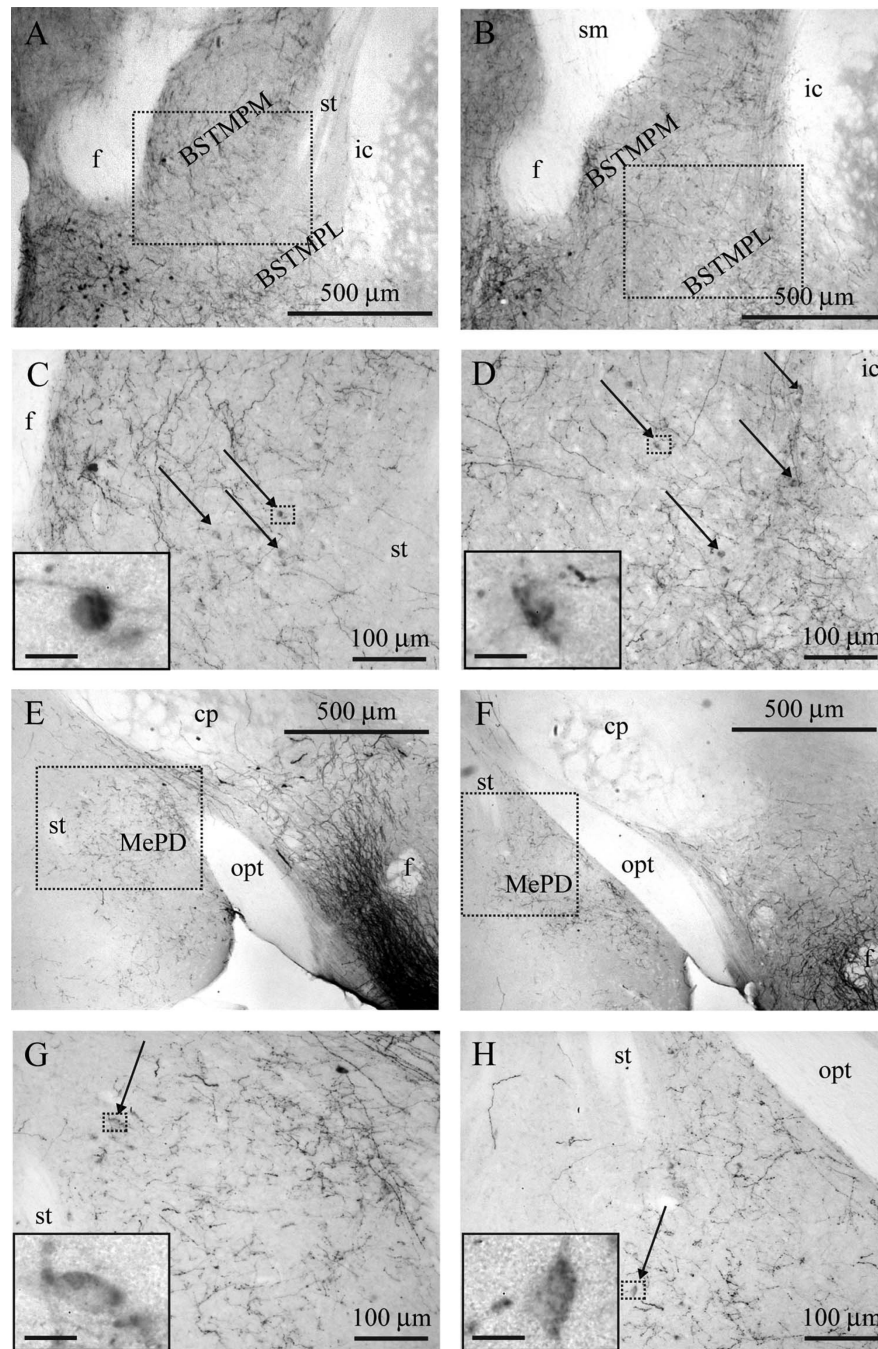


Figure 1. BNST and amygdala. **A:** Bregma -0.10 . Small, lightly staining AVP-ir cells are found above the fibers of the stria terminalis in the medial BSTMPM. **B:** Bregma -0.22 . AVP-ir cells are also found in the BSTMPL slightly caudal and ventral to those in the BSTMPM. **C:** Magnification of the BSTMPM from boxed area in A. **D:** Magnification of the BSTMPL from boxed area in B. **E:** Bregma -1.34 . AVP-ir cells are found at the dorsolateral edge of the rostral MePD. **F:** Bregma -1.46 . AVP-ir cells are found in the caudal MePD as well. **G:** Magnification of the rostral MePD from boxed area in E. **H:** Magnification of the caudal MePD from boxed area in F. In C,D,G,H, arrows indicate AVP-ir cells, and insets depict

individual cells at high magnification. Scale bars = 500 μm in A,B,E,F; 100 μm in C,D,G,H; 10 μm in insets.

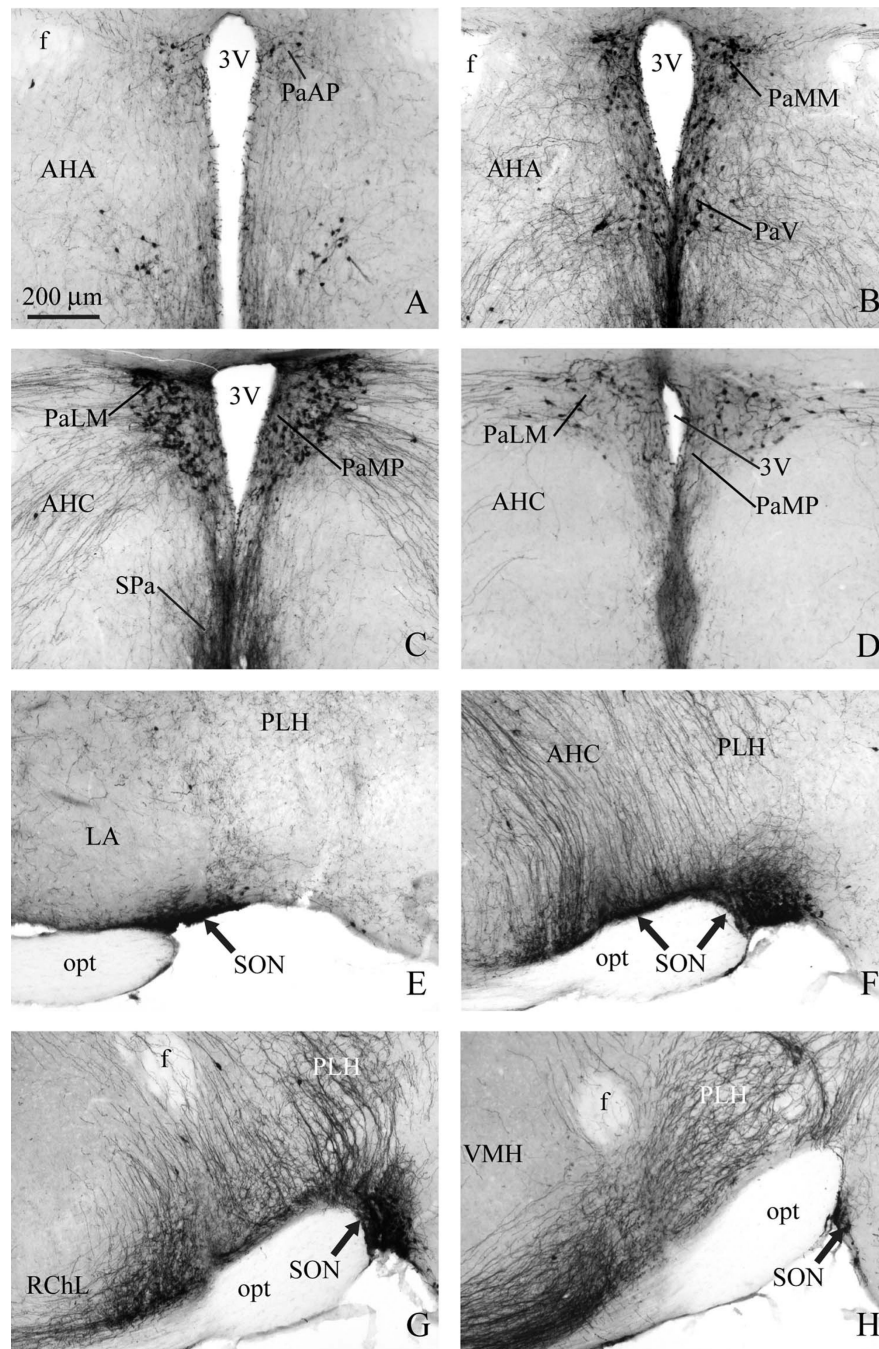


Figure 2. PVN and SON. **A:** Bregma -0.46 . AVP-ir neurons in the PaAP. **B:** Bregma -0.70 . Magnocellular neurons are located close to the third ventricle in the PaMM and PaV. **C:** Bregma -0.82 . Magnocellular neurons in the PaLM, and parvocellular neurons in the PaMP medially near the ventricle. **D:** Magnocellular neurons in the PaLM persist as other cell groups end caudally. **E:** Bregma -0.58 . AVP-ir cells in the episupraoptic nucleus just dorsal to the rostral tip of the optic tract (opt). **F:** Bregma -0.82 . Rostral pole of extremely dense cluster of AVP-ir cells in the SON dorsal and lateral to the optic tract. **G:** Bregma -0.94 . Continuation of dense cluster of AVP-ir cells dorsal and lateral to the lateral edge of the optic

tract, plus AVP-ir cells along the ventral brain surface closer to the midline. **H**: Bregma – 1.06. A few scattered cells lateral to the optic tract at the caudal edge of the SON. Scale bar = 200 μm .

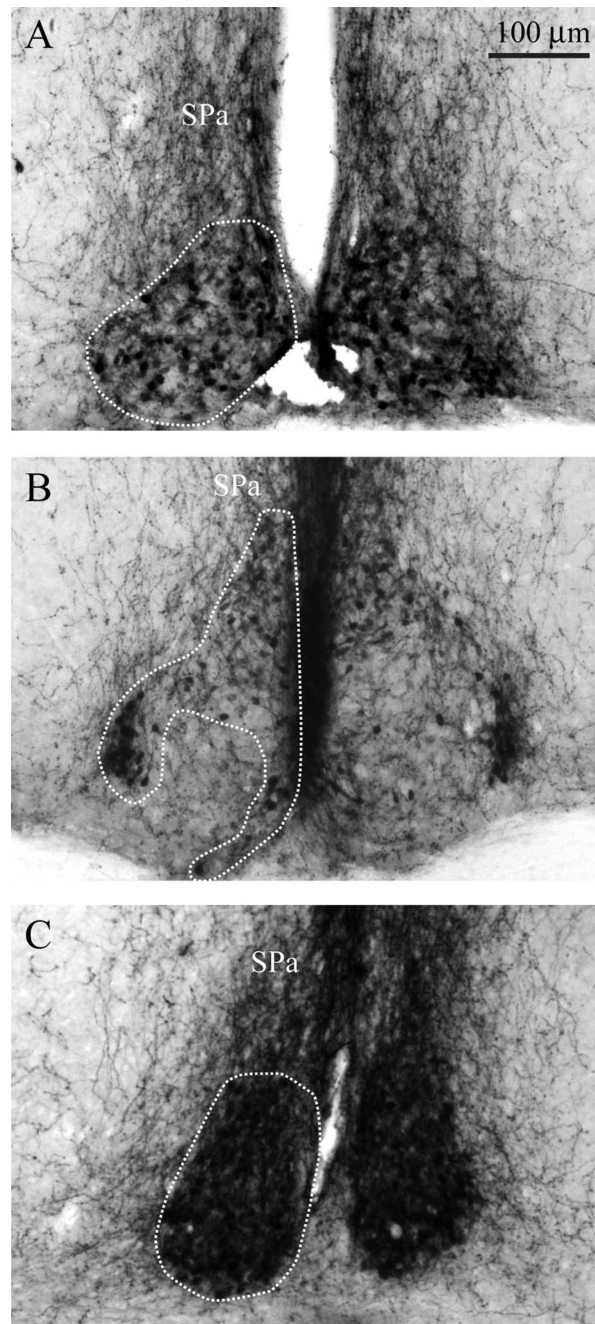


Figure 3. SCN. **A:** Bregma -0.34 . The rostral SCN contains a dense cluster of small, darkly staining cells. **B:** Bregma -0.58 . In the middle SCN, AVP-ir cells in the SCN form a shell around an AVP-ir cell-free core. **C:** Bregma -0.82 . The caudal SCN also has a dense cluster of AVP-ir cells. Outlines illustrate the extent of cells in the SCN. Scale bar = 100 μm .

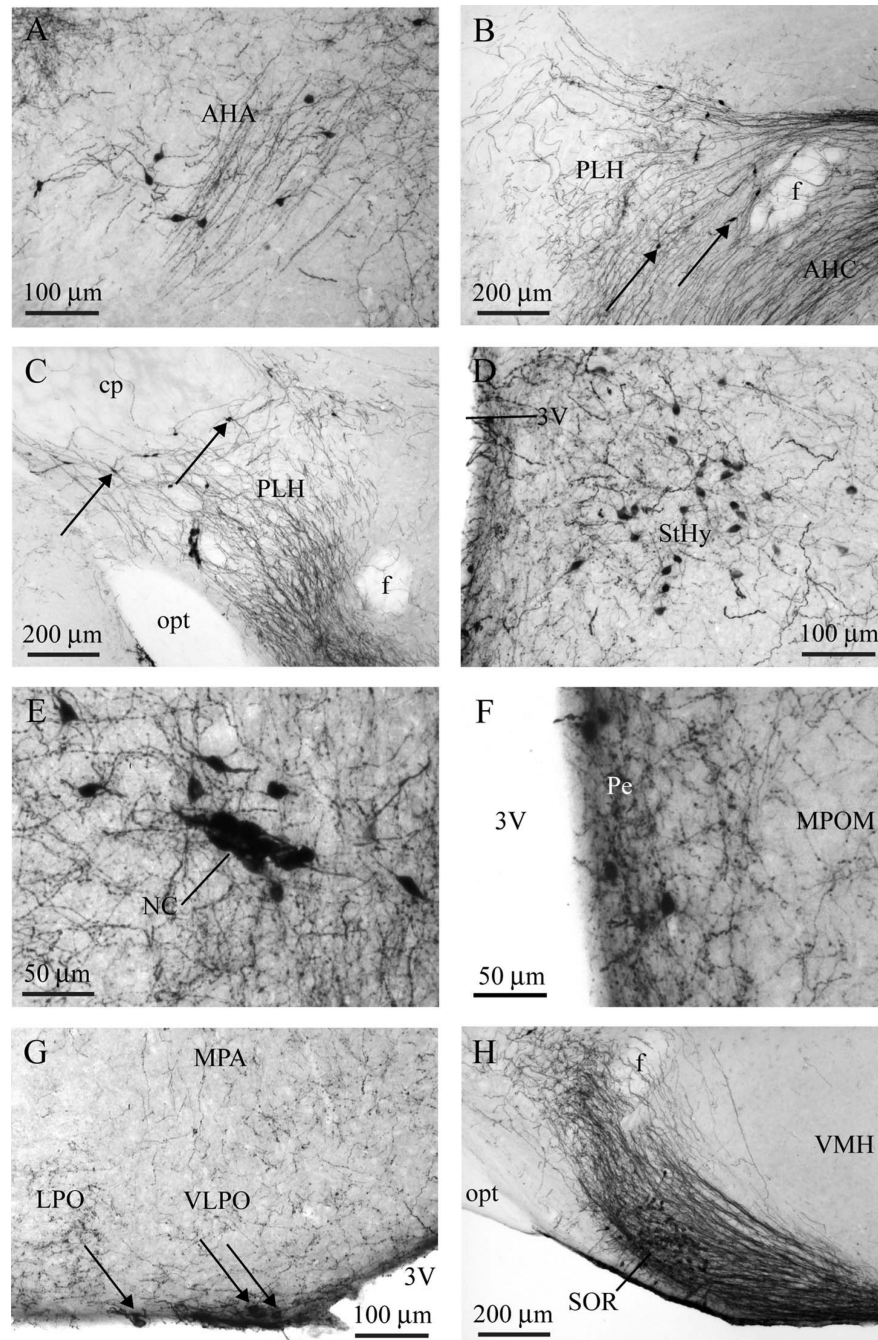


Figure 4. Accessory nuclei and other hypothalamic nuclei. Darkly staining AVP-ir neurons in the rostral anterior hypothalamus (AHA; bregma -0.46 ; **A**), perifornical region (bregma -0.70 ; **B**), peduncular lateral hypothalamus (PLH; bregma -1.22 ; **C**), “mouse accessory nucleus” (Castel and Morris, 1988) in the striohypothalamic region (StHy; bregma -0.22 ; **D**), nucleus circularis (NC; bregma -0.46 ; **E**), rostral periventricular area (Pe; bregma -0.10 ; **F**), ventral lateral preoptic area (VLPO; bregma 0.02 ; **G**), and retrochiasmatic supraoptic nucleus at the level of the tuberal lateral hypothalamus (SOR; bregma -1.46 ; **H**). In all pictures, arrows

indicate representative cells within the picture. Scale bars = 100 μm in A,D,G; 200 μm in B,C,H; 50 μm in E,F.

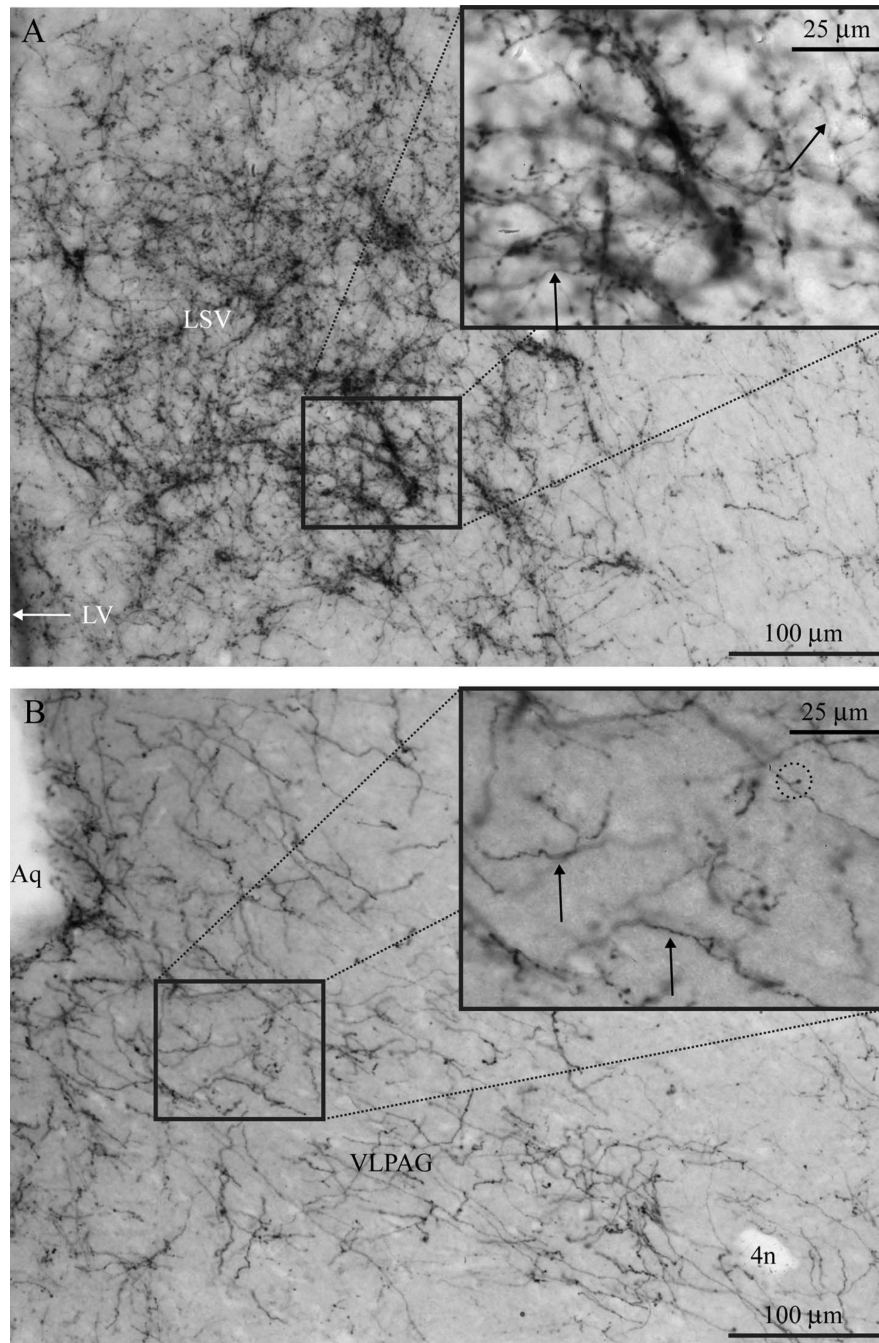


Figure 5. Fiber size. **A:** Bregma 0.38. Small AVP-ir fibers in the LSV with punctate staining. **B:** Bregma -4.72. Medium-sized fibers in the VLPAG with occasional terminal boutons with visible stalks (see circled structure in B). In each figure, arrows indicate representative fibers. Scale bars = 100 µm in A,B; 25 µm in insets.

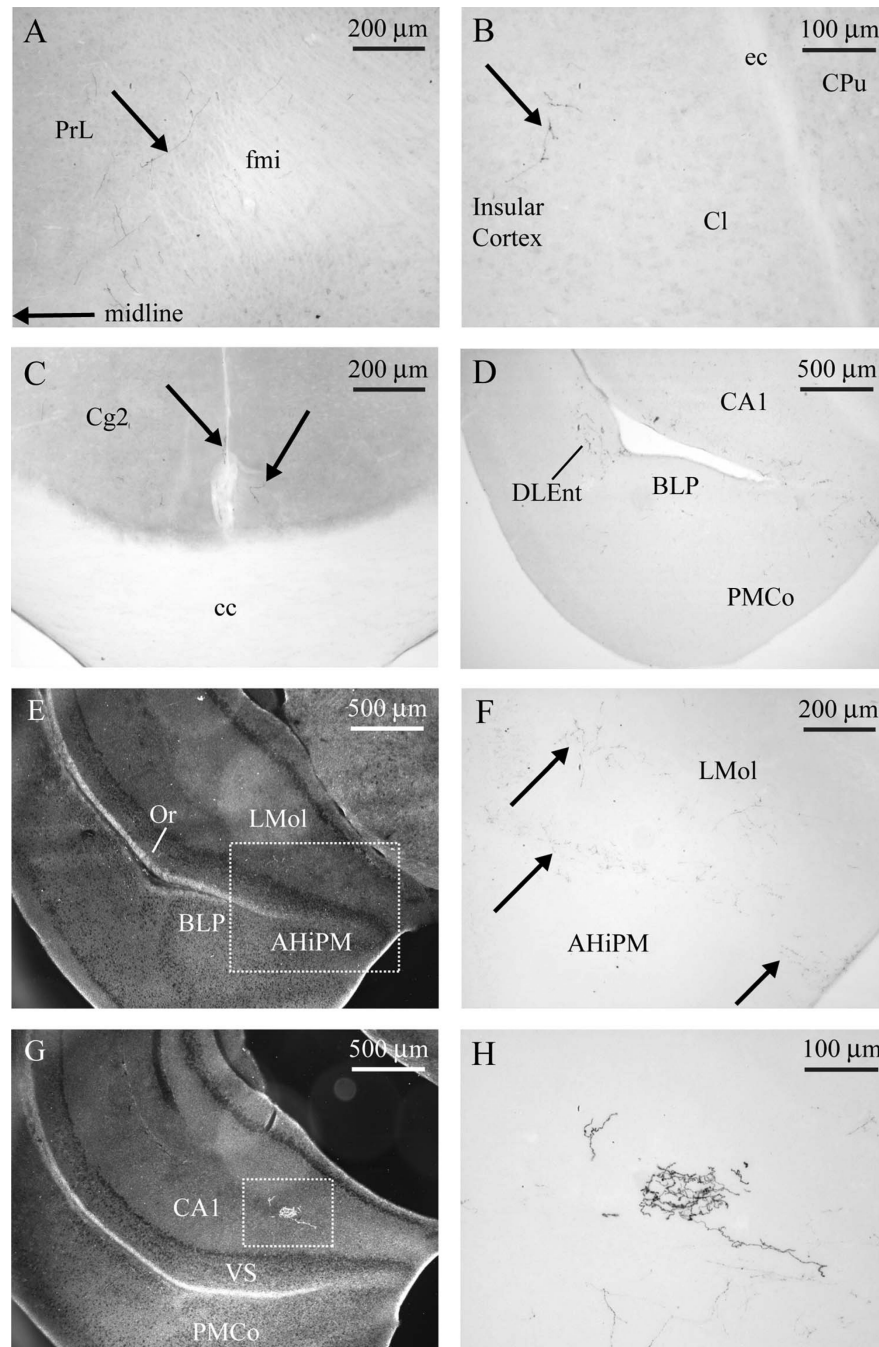


Figure 6. Cortex and hippocampus. **A–C:** Sparse medium-sized AVP-ir fibers in the the PrL (bregma 1.98; **A**), insular cortex (bregma – 0.10; **B**), and Cg2 (bregma 1.10; **C**). **D:** Bregma –2.54. Small fibers are seen in more caudal regions of the cortex, especially the DLEnt. **E:** Bregma –2.92. Darkfield image of CA1 region of the ventral hippocampus. **F:** Brightfield image showing small fibers from boxed area in **E**. **G:** Bregma –3.28. Darkfield image of CA1 region of the ventral hippocampus. **H:** Brightfield image showing medium-sized fibers from boxed area in **G**. Scale bars = 200 μm in **A,C,F**; 100 μm in **B,H**; 500 μm in **D,E,G**.

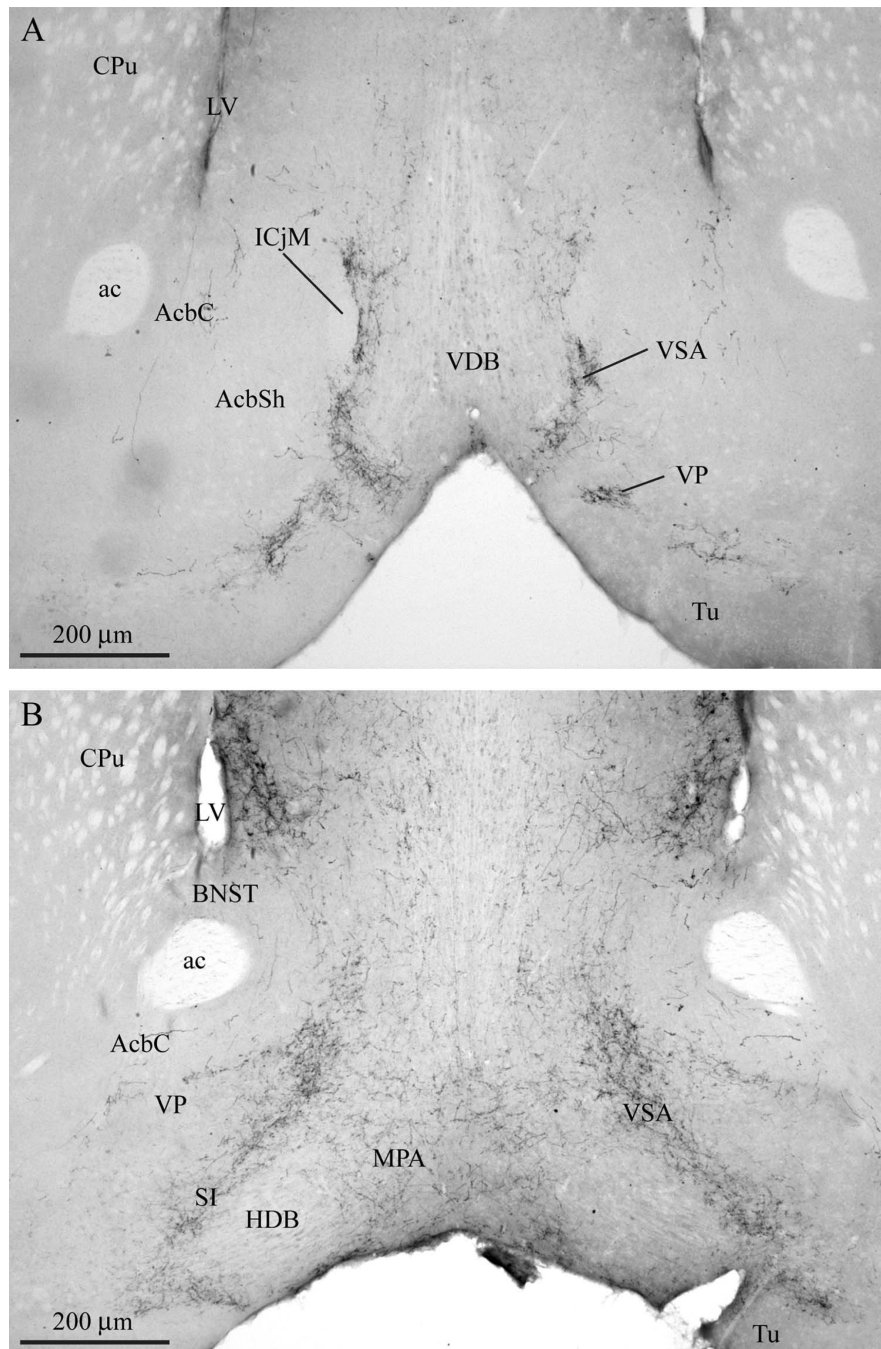


Figure 7. Basal ganglia and ventral forebrain. **A:** Bregma 0.98. Small AVP-ir fibers in the VP and the ventral septal area (VSA) between the AcbSh and VDB in the rostral forebrain. Medium-sized fibers are found in the AcbC. **B:** Bregma 0.6. Small fibers in the MPA, VP, SI, and VSA. AVP-ir fibers avoid the VDB, ICjM, Tu, and AcbSh. Scale bars = 200 μm.

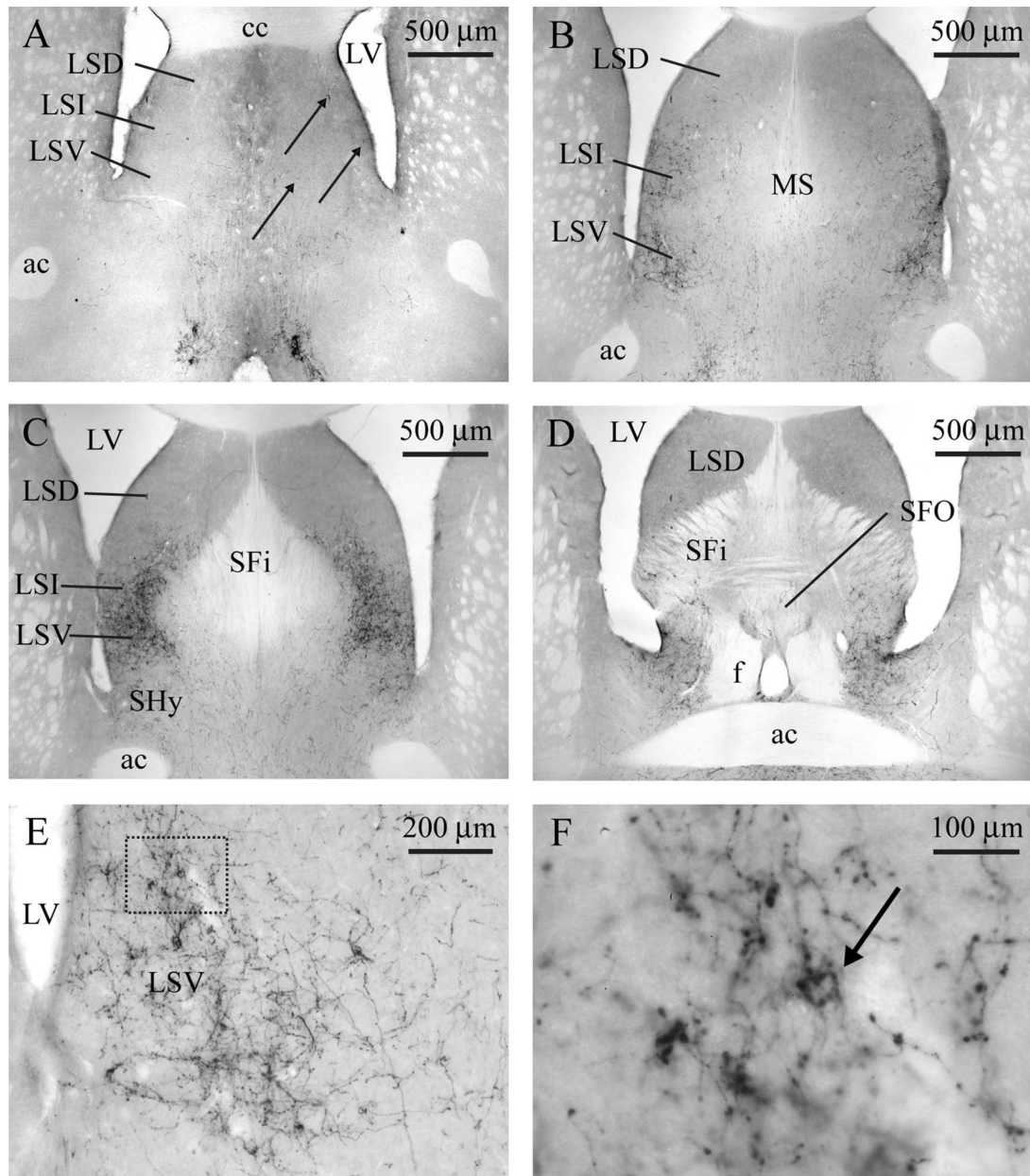


Figure 8.

Septal complex. **A:** Bregma 0.86. Sparse medium-sized AVP-ir fibers in the rostral LS. **B:** Bregma 0.62. Small fibers in the LSV and LSI. **C:** Bregma 0.38. Very dense small fiber innervation of the caudal part of the LSV and LSI. **D:** Bregma -0.1. Isolated small fibers in the SFi and medium-sized fibers in the SFO. **E:** Magnification of the LSV from B. **F:** High magnification of boxed area in E. The arrow identifies a pericellular basket. Scale bars = 500 μm in A-D; 200 μm in E; 100 μm in F.

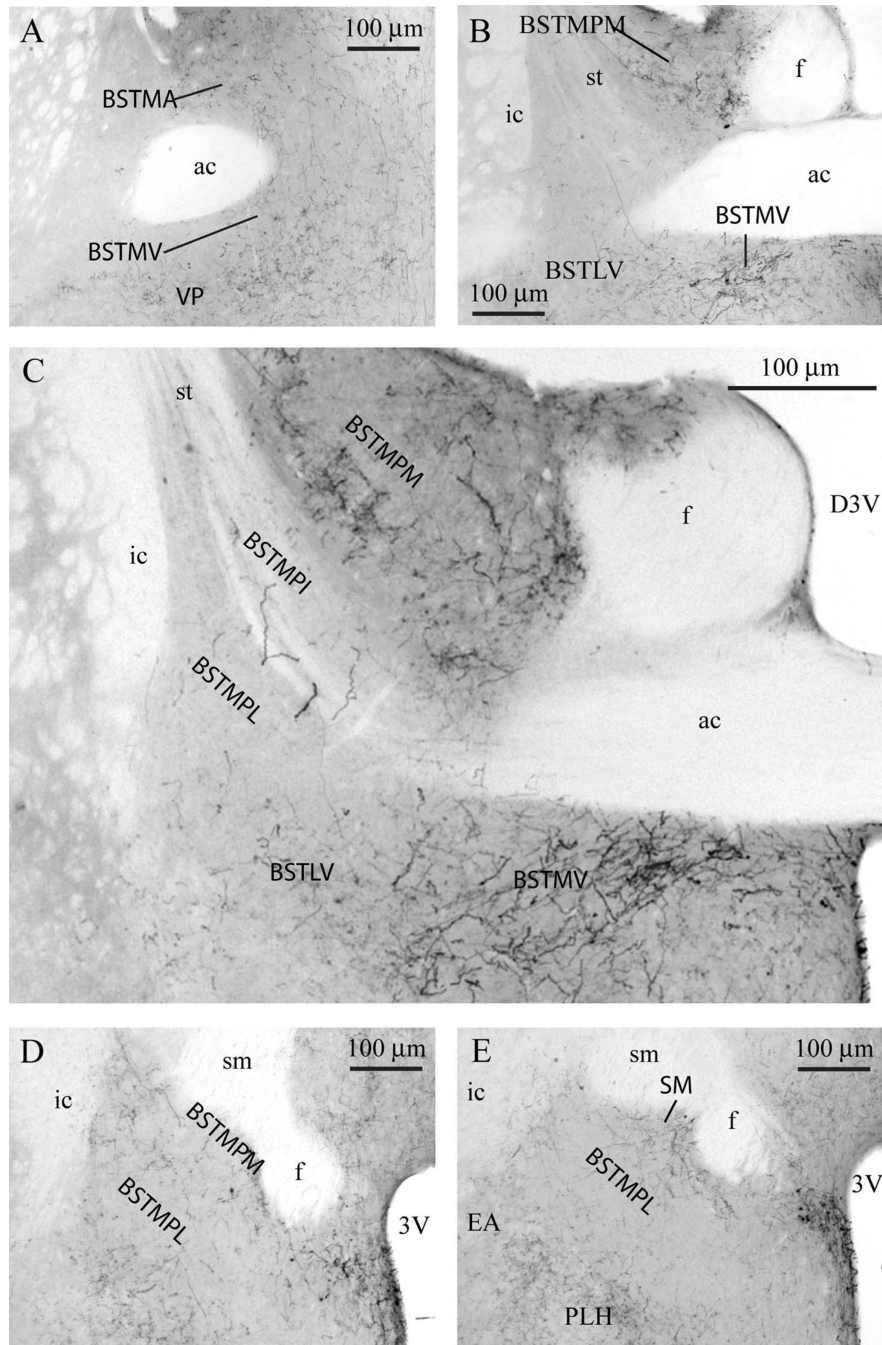


Figure 9.

Bed nucleus of the stria terminalis. **A:** Bregma 0.50. Small and medium-sized AVP-ir fibers in the BSTMA and medium-sized fibers in the BSTMV. **B:** Bregma 0.02. Small fibers in the BSTLV and medium-sized fibers in the BSTMV. **C:** Bregma -0.10. Two distinct clusters of small fibers and a number of medium-sized fibers in the BSTMPM, small fibers in the BSTLV, and medium-sized fibers in the BSTMV. **D:** Bregma -0.34. BSTMPL with BNST cells in the BSTMPL and small fibers, which can be seen entering the stria terminalis (st). **E:** Bregma -0.46. Dense small fibers ventral to stria medullaris (sm), but less dense in the rest of the BNST. Scale bars = 100 µm.

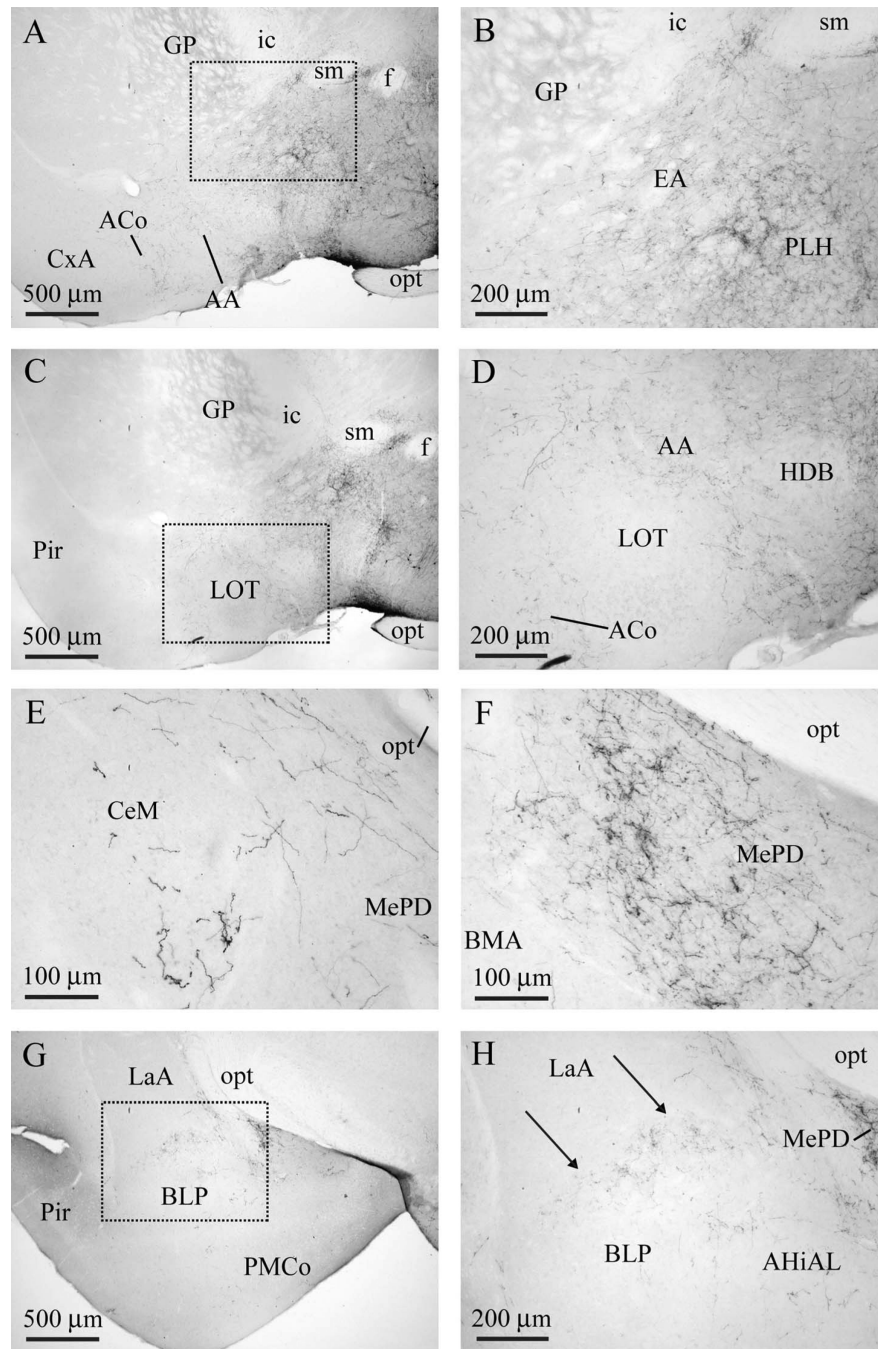


Figure 10.

Amygdala. **A:** Bregma -0.58 . Diffuse small fibers in the AA and EA (see footnote 1). **B:** Magnification from boxed area in A showing moderate numbers of fibers in the EA and a denser plexus in the neighboring PLH. **C:** Bregma -0.7 . Small fibers in the EA, AA, and ACo but not in the LOT. **D:** Magnification from boxed area in C. **E:** Bregma -1.3 . Medium-sized fibers in CeA. **F:** Bregma -1.58 . A dense small fiber plexus is found in the MePD. **G:** Bregma -2.18 . Small fibers in the caudal BLP just ventral to the LA. **H:** Magnification from boxed area in G showing fibers in the BLP. Scale bars = $500\ \mu\text{m}$ in A,C,G; $200\ \mu\text{m}$ in B,D,H; $100\ \mu\text{m}$ in E,F.

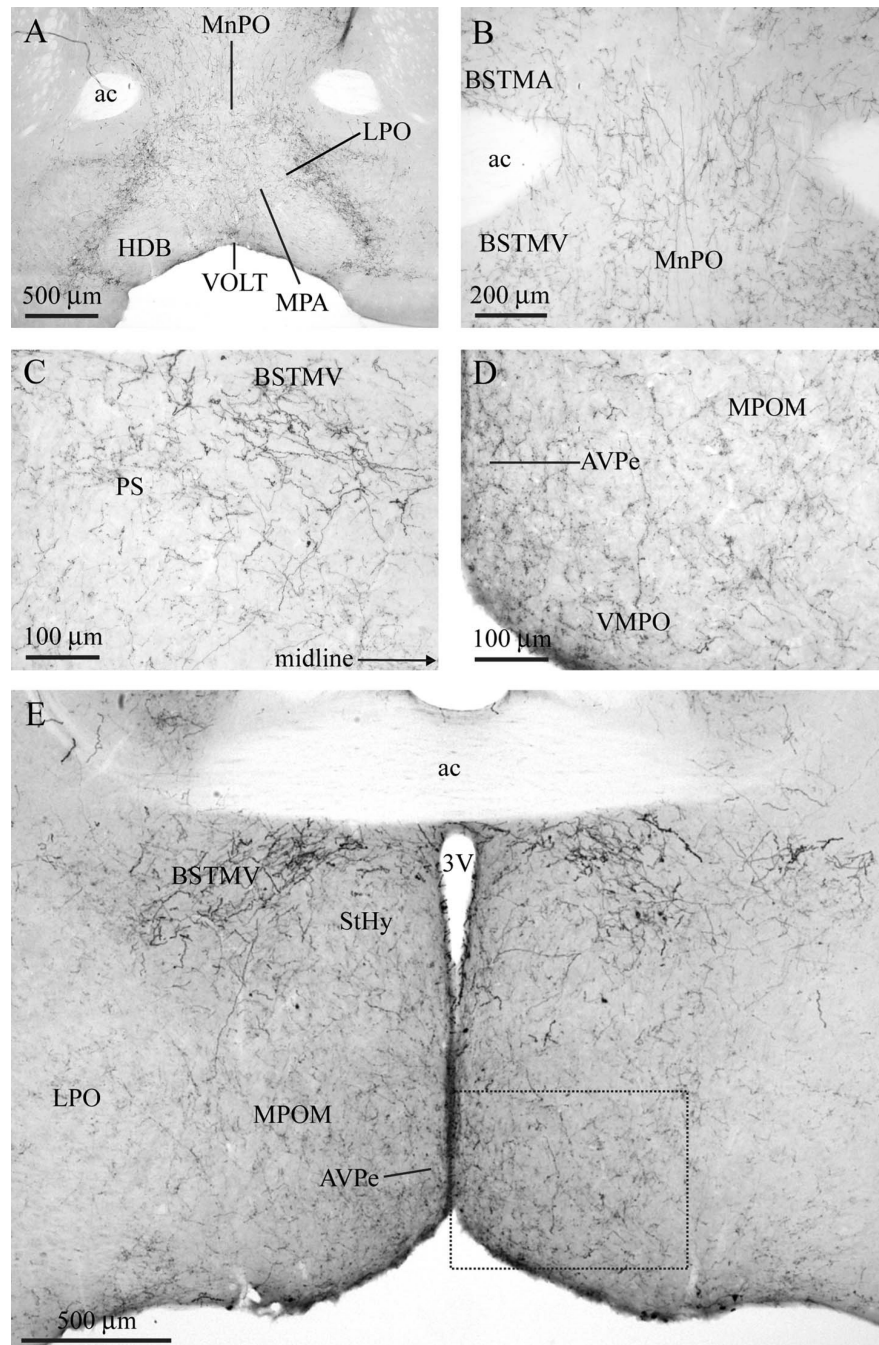


Figure 11.

Preoptic area. **A:** Bregma 0.38. Small AVP-ir fibers in the MPA and medium-sized fibers in the VOLT and MnPO. **B:** Bregma 0.26. MnPO at higher magnification. Medium-sized fibers are oriented vertically in the plane of section. **C:** Bregma 0.14. Dense small fiber plexus in the PS ventral to the BSTMV. **D:** Magnification of boxed area in E showing scattered small and medium-sized fibers in the MPOM, and many small fibers and some medium-sized fibers in AVPe. **E:** Bregma -0.10. Sparse small and medium-sized fibers in the caudal LPO and StHy. Scale bars = 500 μm in A,E; 200 μm in B; 100 μm in C,D.

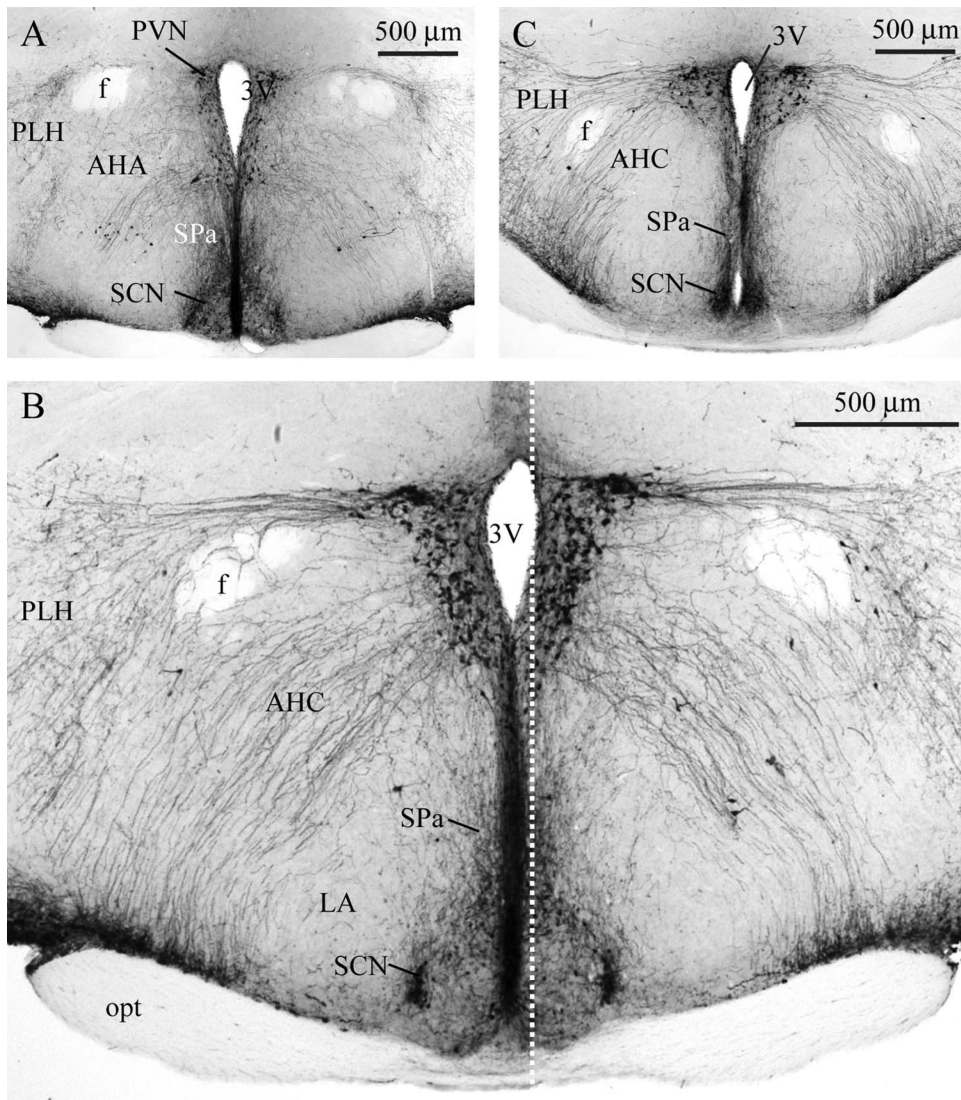


Figure 12. Anterior hypothalamus. **A:** Bregma -0.58 . Small fibers in the AHA ventral to the fornix and dorsal to the SCN adjacent to third ventricle and medium-sized fibers stretching between the PVN and SON through ventral parts of the AHA. **B:** Bregma -0.82 . Small fibers are found medially in the SCN, SPa, and PVN. Medium-sized fibers dominate the AHC and numerous medium-sized fibers pass over the fornix into the PLH. **C:** Bregma -0.94 . Caudally, fewer medium-sized fibers pass through the AHC, but many still pass into the PLH. Large amounts of small fibers are still found along the third ventricle. The dotted line indicates the approximate location of the sagittal section shown in Figure 13. Scale bars = $500\ \mu\text{m}$.

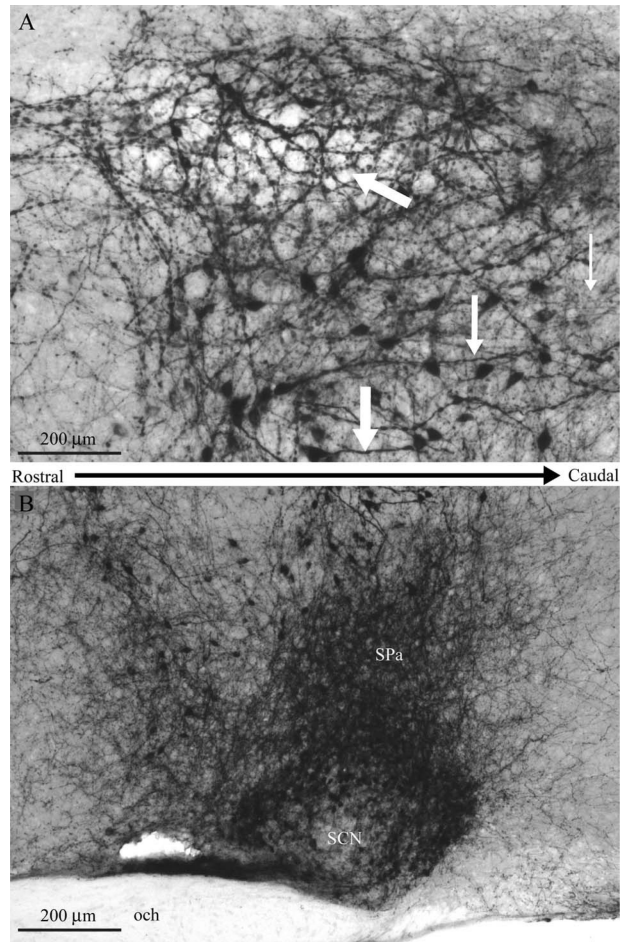


Figure 13. Sagittal section of hypothalamus immediately lateral to the third ventricle (see dotted line in Fig. 12 for approximate location). **A:** Large, medium-sized, and small fibers can be seen among the many PVN neurons adjacent to the third ventricle (large, medium-sized, and small vertical arrows indicate fibers of each type). The last white arrow identifies a lighter region that corresponds to the third ventricle. **B:** In the same sagittal section, a dense cloud of small fibers is seen in and around the SCN. Fibers can be seen passing in all direction, with the largest groups passing dorsally, dorsocaudally, and rostradorsally. Scale bars = 200 μm.

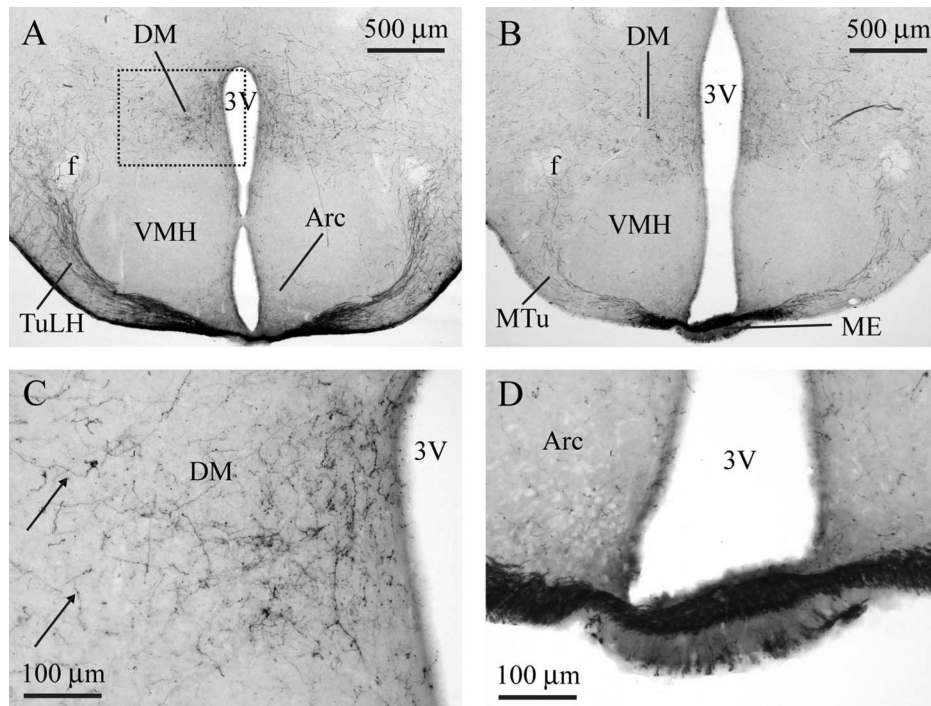


Figure 14.

Dorsomedial hypothalamus. **A:** Bregma -1.46 . Small and medium-sized fibers in the DM and Arc, medium-sized fibers in the TuLH, and a near absence of fibers in the VMH. **B:** Bregma -1.82 . Small and medium-sized fibers in the DM. **C:** Magnification of DM from boxed area in A. Note small punctate staining closer to 3V and numerous medium-sized fibers (arrows). **D:** Magnification of the ME from B. Note dense staining in dorsal ME (inner zone) and less dense staining in the ventral ME (outer zone). Scale bars = $500\ \mu\text{m}$ in A,B; $100\ \mu\text{m}$ in C,D.

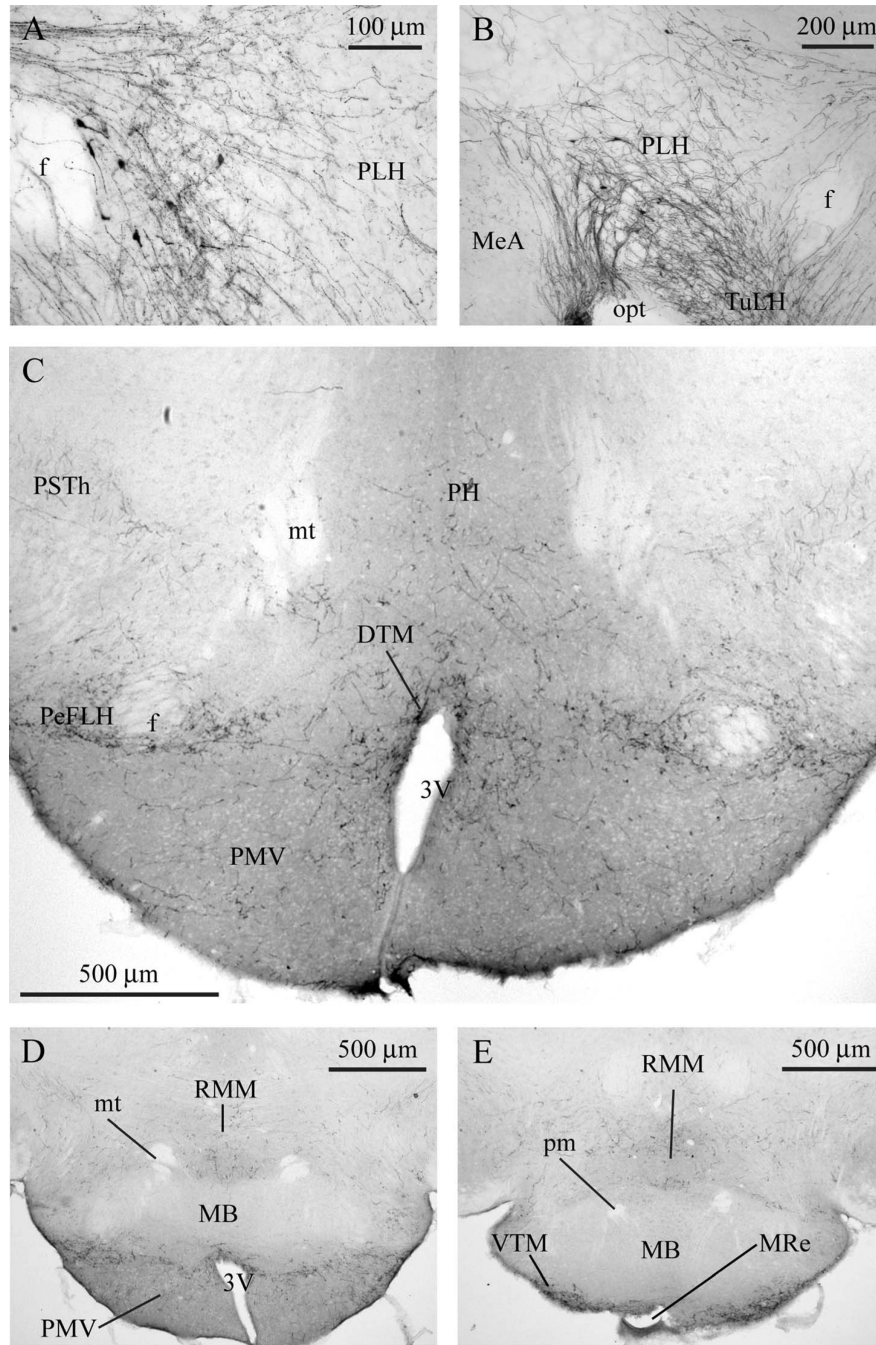
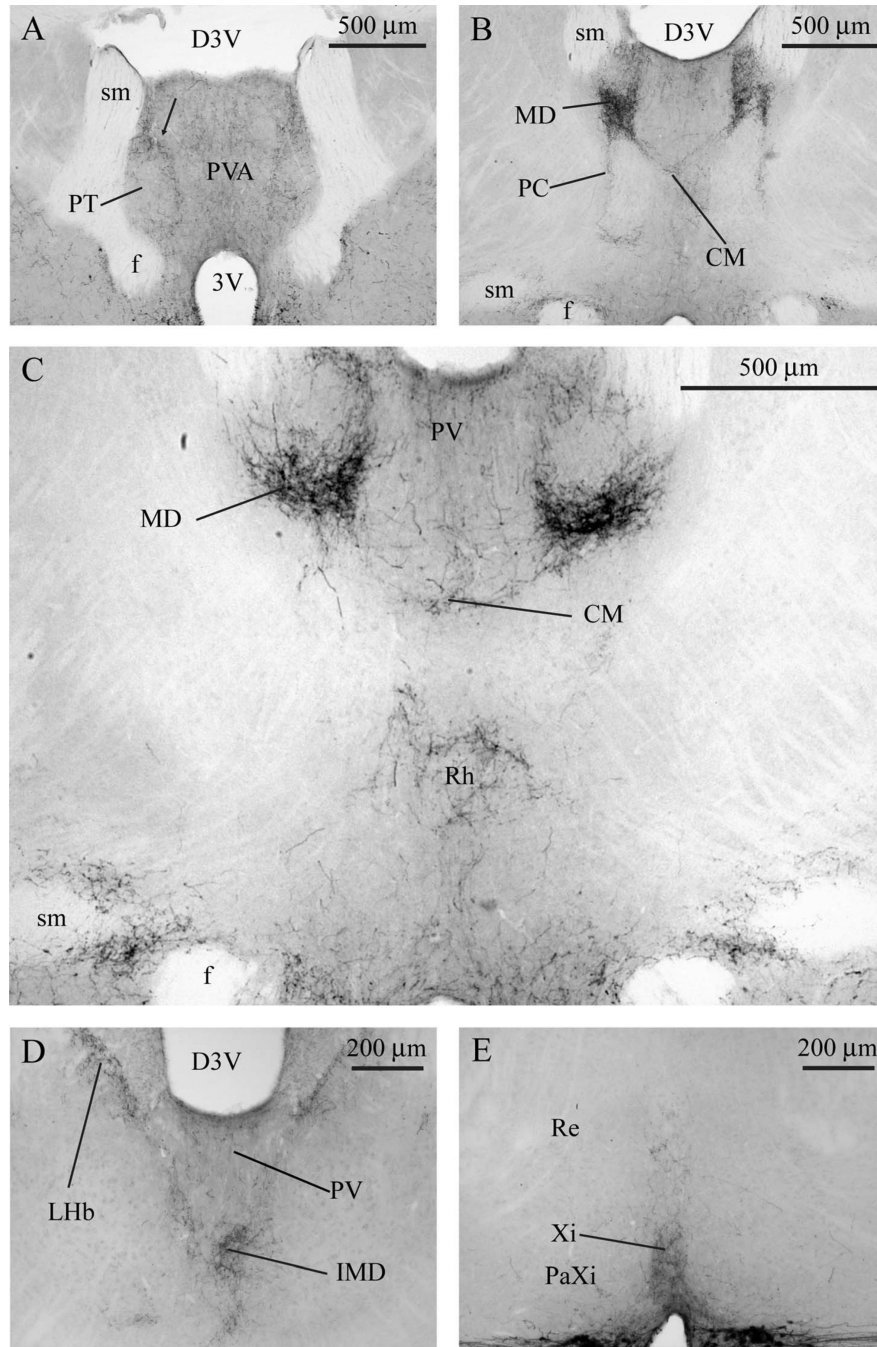


Figure 15.

Lateral hypothalamus and mammillary bodies. **A:** Bregma -0.82 . Small fibers among medium-sized fibers passing through the PLH. **B:** Bregma -1.2 . Fewer small fibers are seen in the caudal PLH, but a dense array of medium-sized and large fibers is observed. **C:** Bregma -2.46 . Small fibers in the PeFLH and DTM around the fornix (f). Scattered small and medium-sized fibers in the PMV, PH, and PSTh. **D:** Bregma -2.54 . Dense plexus of small fibers just ventral to the MB, small and medium-sized fibers in RMM, scattered small fibers in the PMV, and absence of fibers in MB. **E:** Bregma -2.80 . Dense plexus of small

fibers in the VTM and scattered small and medium-sized fibers in the RMM. Scale bars = 100 μm in A; 200 μm in B; 500 μm in C–E.



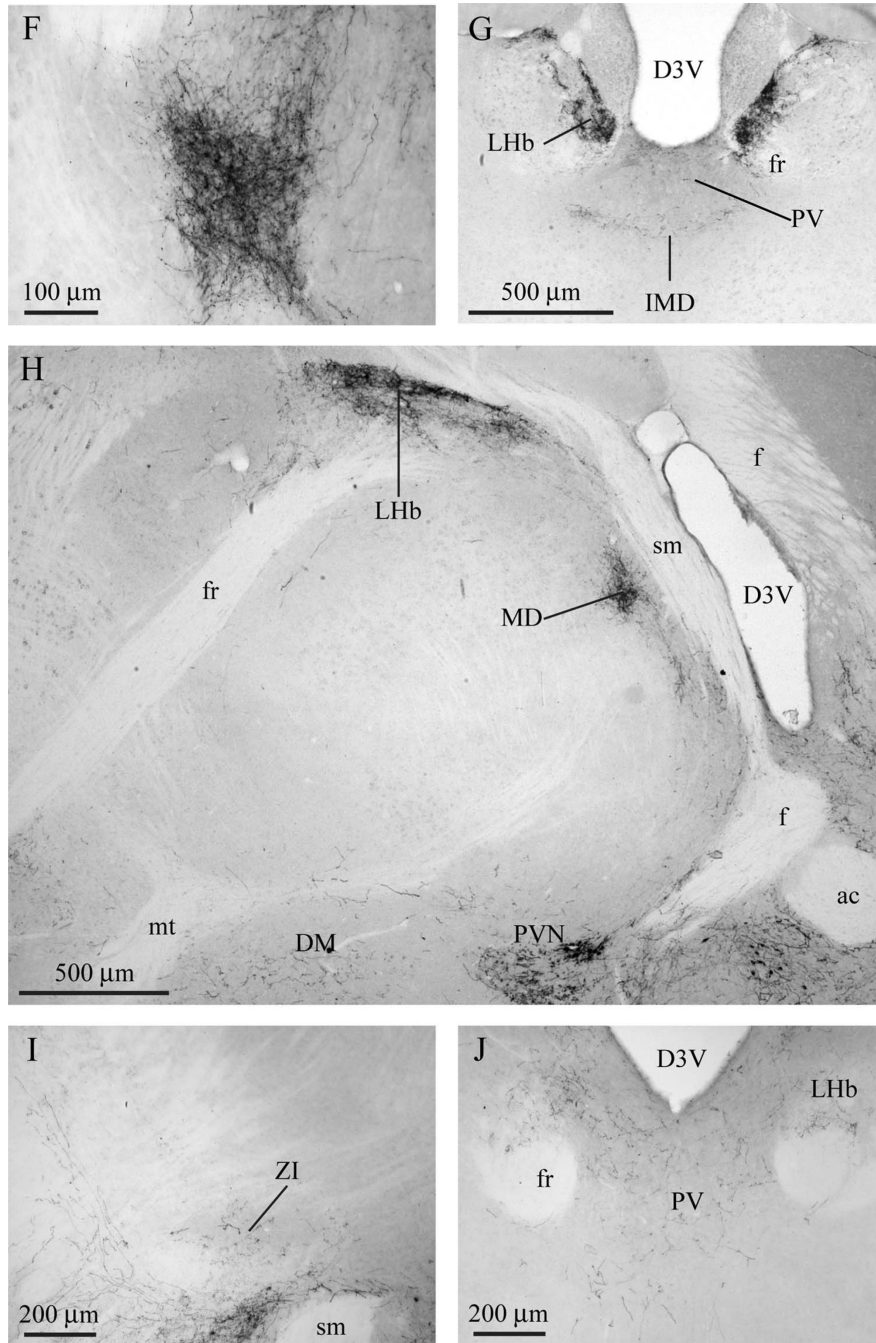
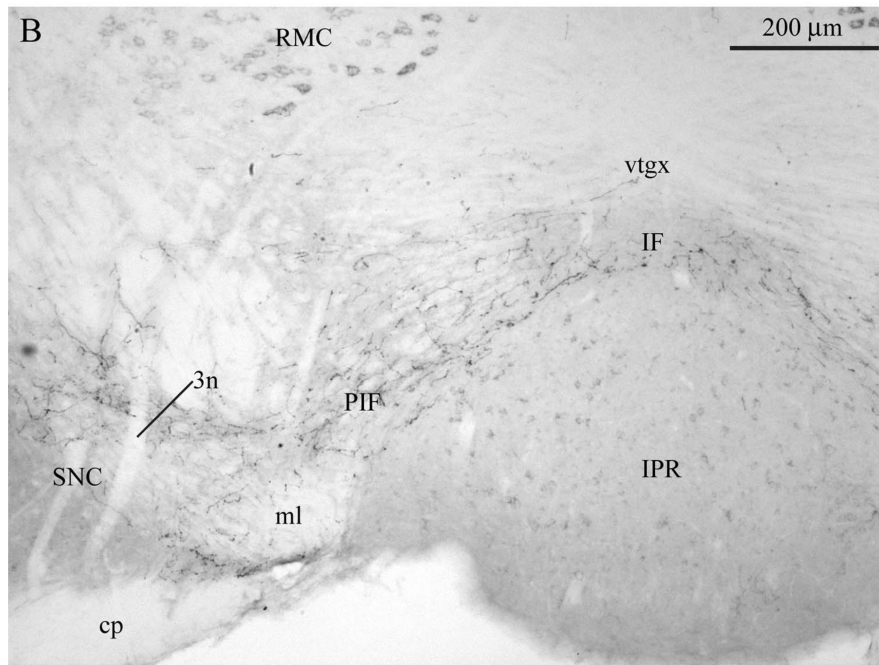
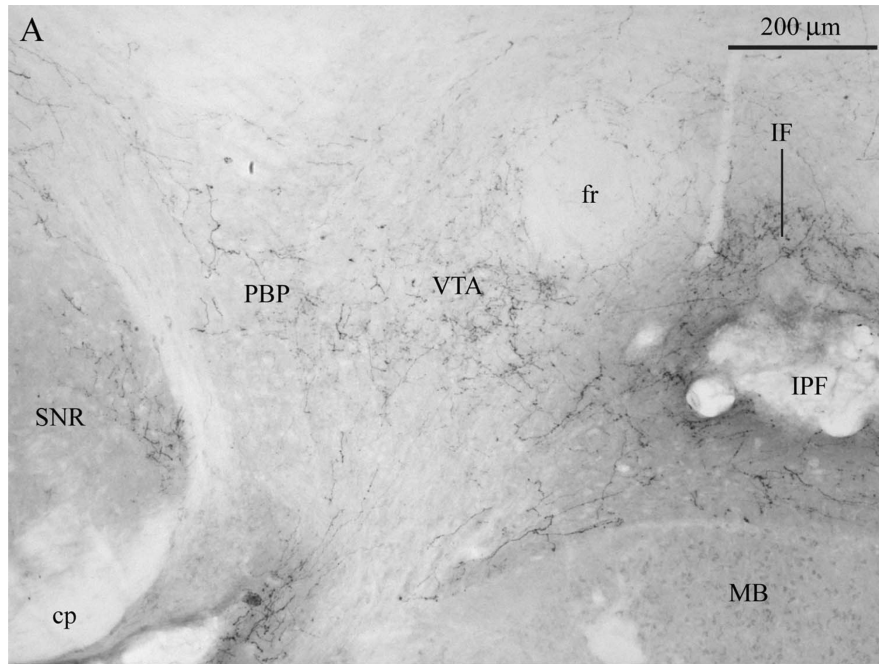


Figure 16.

Thalamus. **A:** Bregma -0.34 . Small fibers in the PVA and periphery of the PT, Arrow points at a dense cluster of fibers dorsal to the PT. **B:** Bregma -0.58 . Dense plexus of small fibers in the MD and additional fibers in the CM and PC surrounding the PT. **C:** Bregma -0.94 . Dense plexus of small fibers in the MD and additional small fibers in the PV, CM, and Rh. Medium-sized fibers in the PV and Rh. **D:** Bregma -1.22 . Small fibers in the LHb and IAD and in the PV just ventral to the dorsal aspect of the third ventricle. **E:** Bregma -1.2 . Small fibers in the Xi just dorsal to the third ventricle. **F:** Magnification of MD from B illustrates density of fibers in this region. **G:** Bregma -1.58 . Dense cluster of small fibers in the LHb,

with light innervation of the PV and IMD. **H**: A sagittal section (lateral 0.48 mm) shows the pathway of AVP-ir fibers arching dorsally just ventral to the stria medullaris, with dense fiber plexuses in the LHb and MD. **I**: Bregma -0.58 . Small fibers in the ZI. **J**: Bregma -1.8 . Scattered small fibers in the caudal extent of the LHb, with primarily medium-sized fibers in the PV. Scale bars = $500\ \mu\text{m}$ in A–C,G,H; $200\ \mu\text{m}$ in D,E,I,J; $100\ \mu\text{m}$ in F.



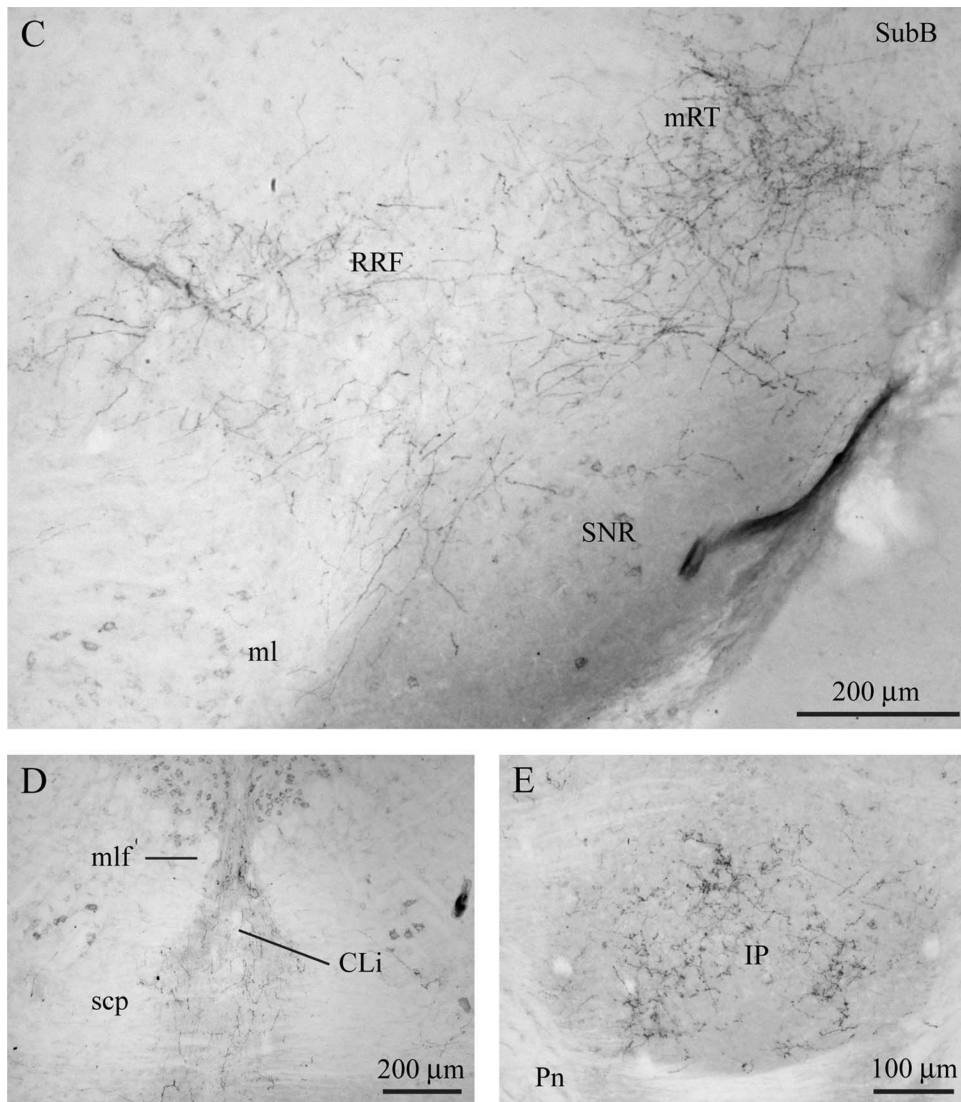
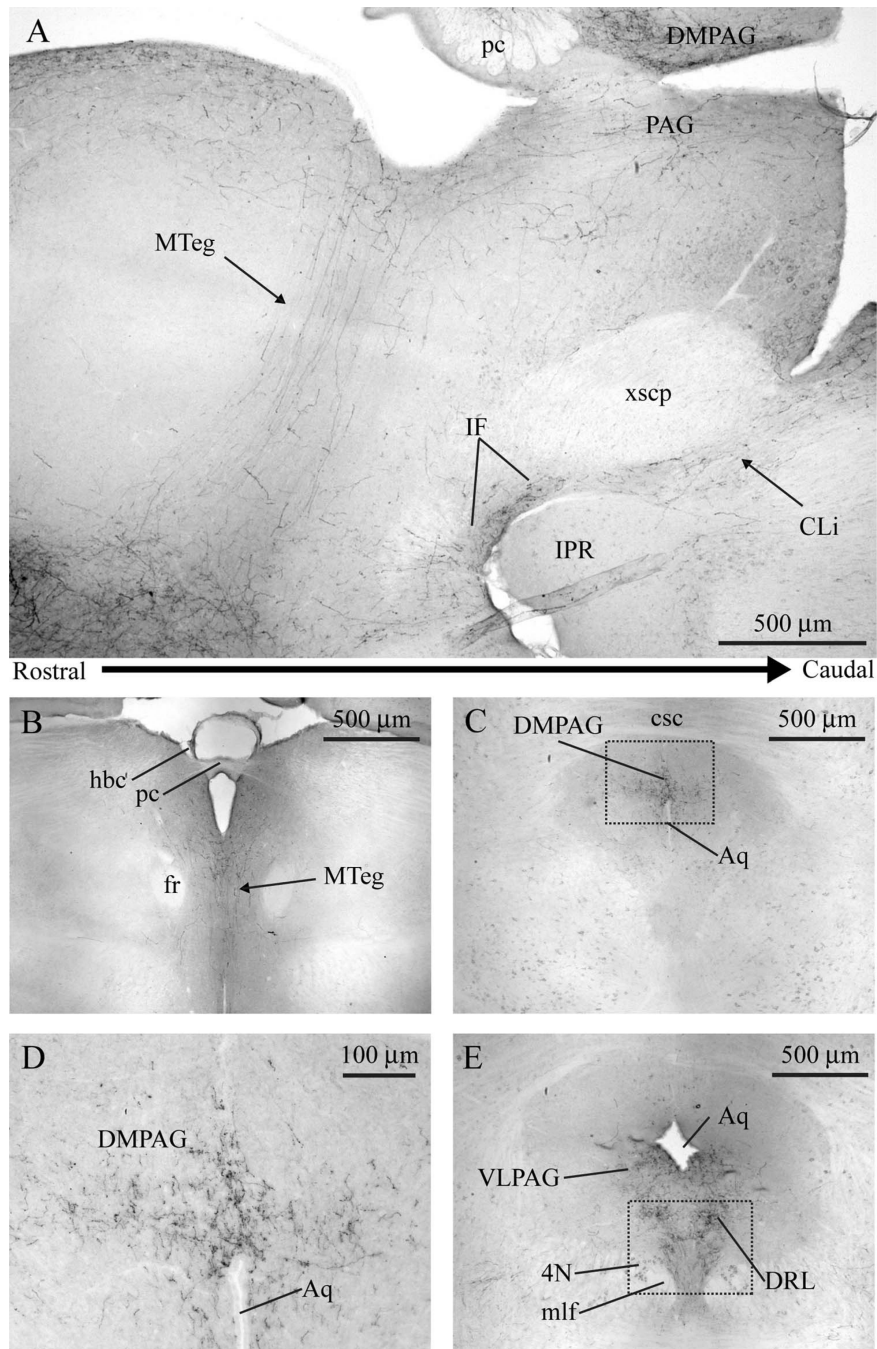


Figure 17. Tegmentum. **A:** Bregma -3.08. Small and medium-sized fibers in the VTA, IF and ventromedial pole of the SNR. **B:** Bregma - 3.52. Small fibers surrounding the IPR in the IF and PIF. **C:** Bregma -4.04. Dense plexus of medium-sized fibers and isolated small fibers in the caudal tegmentum in the mRt and RRF just dorsal to the SNR. **D:** Bregma -4.04. Predominantly small fibers in the CLi between the superior cerebellar peduncles (scp). **E:** Bregma -4.04. Moderate numbers of small fibers in the caudal pole of the IP. Scale bars = 200 μm in A-D; 100 μm in E.



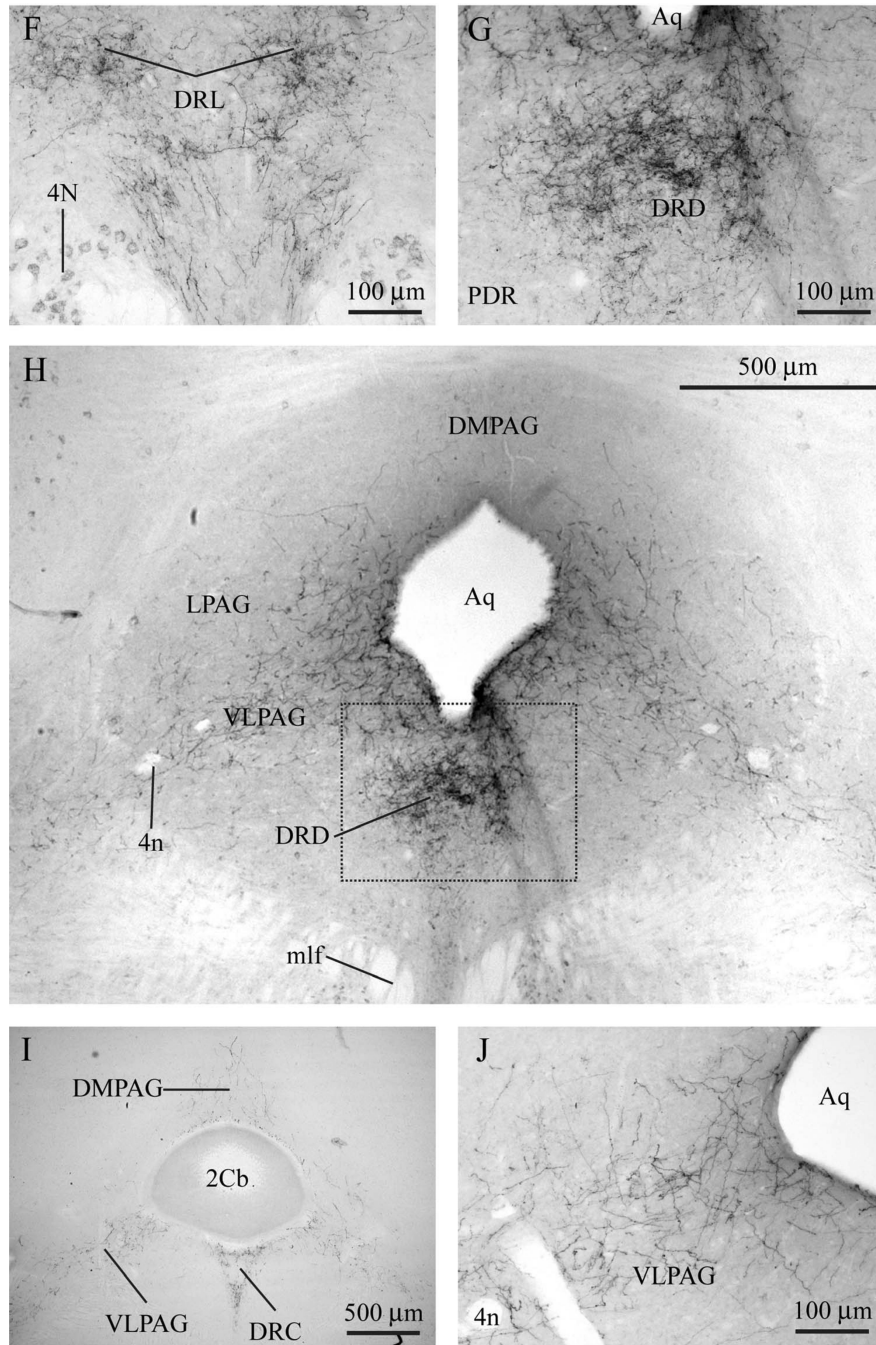


Figure 18.

Periaqueductal gray and dorsal raphe nuclei. **A:** Sagittal section near the midline showing AVP-ir pathways travelling dorsally toward the PAG through the rostral midbrain (left arrow) and caudally through the IF and CLi (right arrow) toward the DR. **B:** Bregma -2.30 . Small and medium-sized fibers ascend dorsally between the right and left fasciculus retroflexus (fr) immediately rostral to PAG. **C:** Bregma -3.52 . Plexus of small fibers in the DMPAG. **D:** Magnification of small fibers in the DMPAG from boxed area in C. **E:** Bregma -4.36 . Dense clusters of small fibers in the DRL and network of medium-sized fibers in the VLPAG. **F:** Magnification of the boxed area in E showing bilateral plexuses in DRL. **G:**

Magnification of the boxed area in H showing a single midline plexus in DRD. **H**: Bregma – 4.60. Dense plexus of small fibers in the DRD at the midline. Medium-sized fibers in a dorsomedial to ventrolateral orientation in the VLPAG. **I**: Bregma –5.02. Small fibers in the DRC and medium-sized fibers in the VLPAG. Note that some medium-sized fibers also enter the DMPAG at this point. **J**: Magnification of medium-sized fibers in the VLPAG. Scale bars = 500 μm in A–C,E,H,I; 100 μm in D,F,G,J.

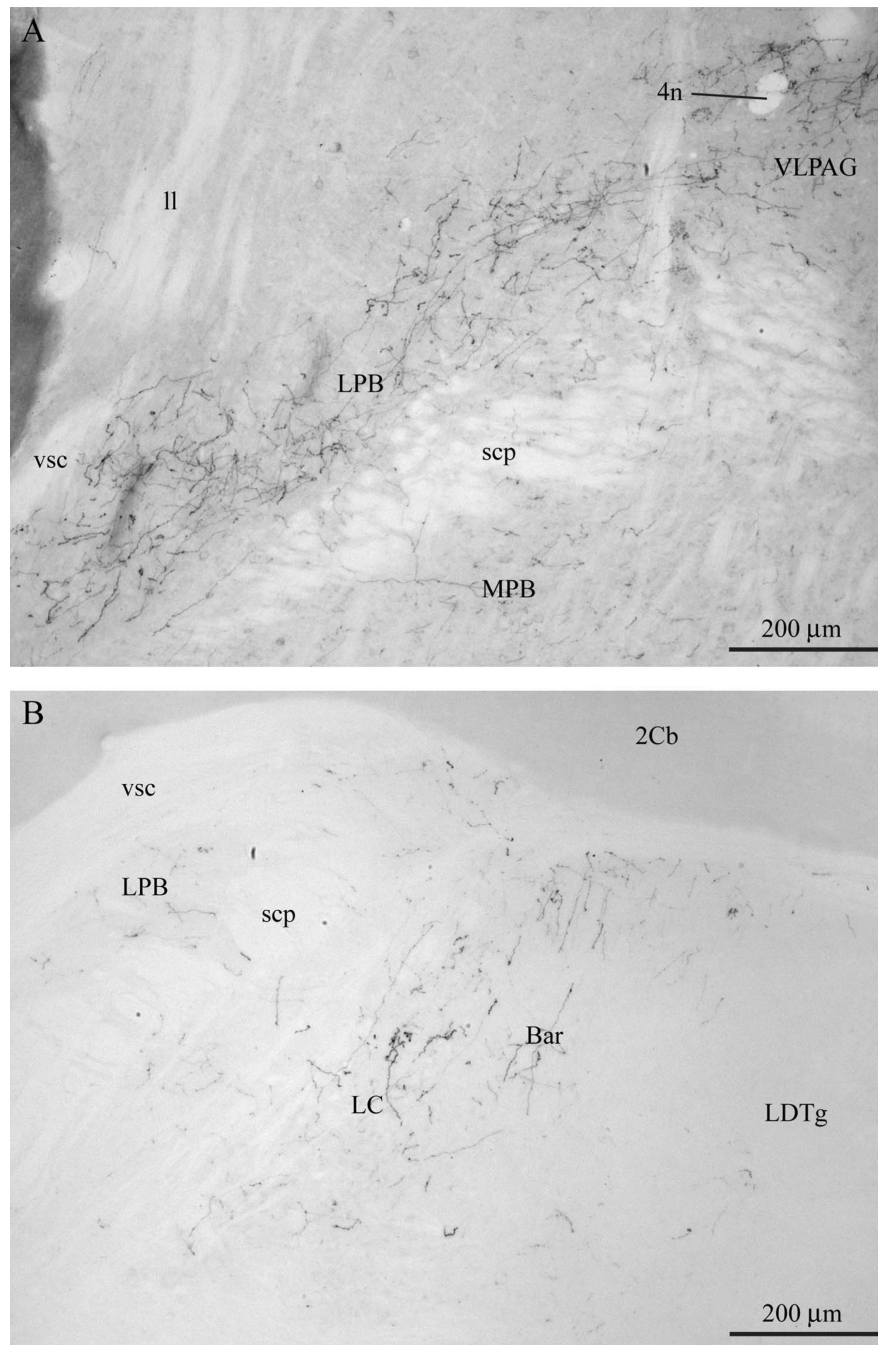
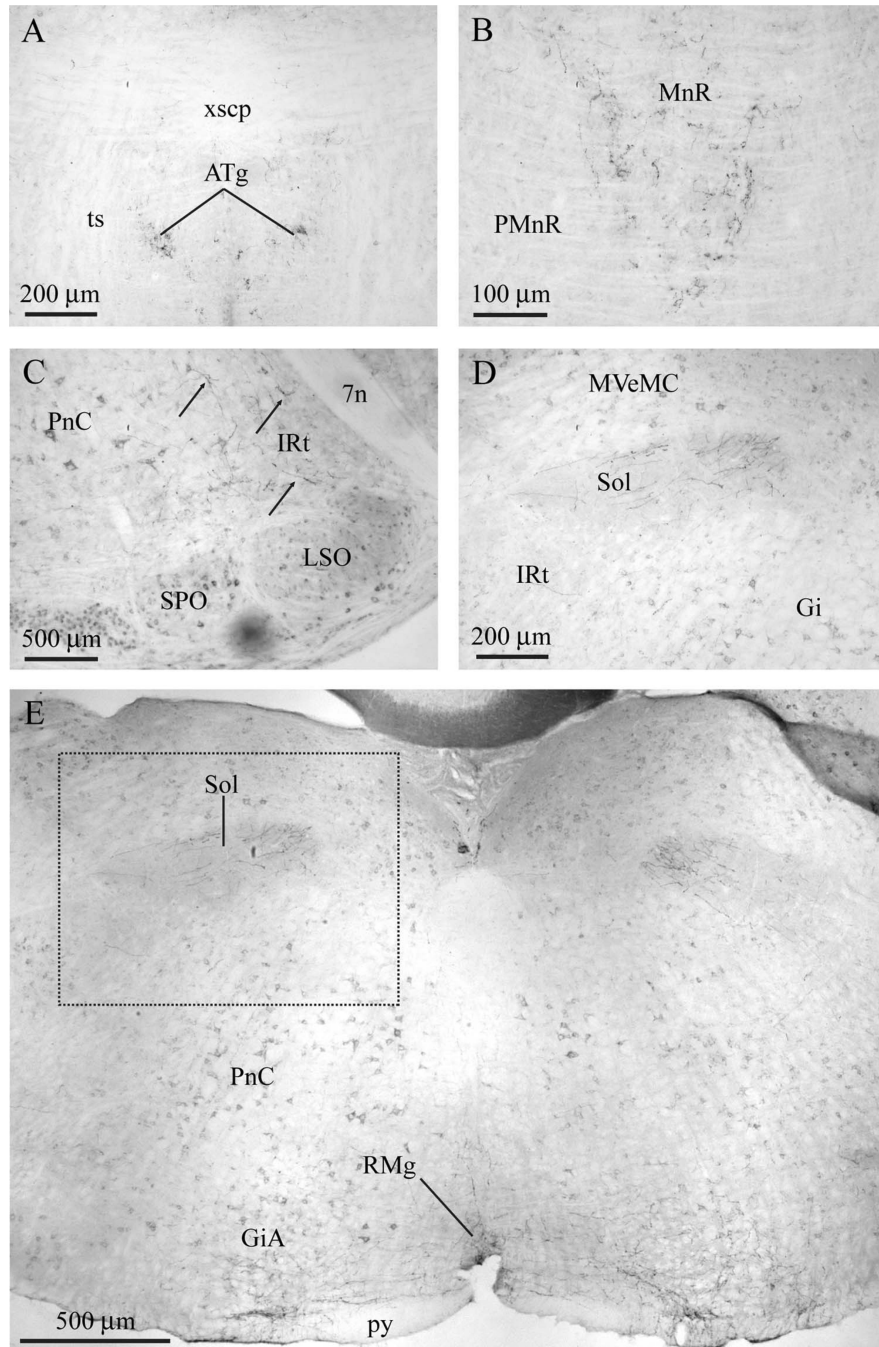


Figure 19. Caudal mesencephalic nuclei. **A:** Bregma -5.02 . Medium-sized fibers stretching from the VLPAG to the LPB and sparse medium-sized fibers in the MPB. **B:** Bregma -5.52 . Medium-sized fibers in the caudal LPB, LC, and Bar. Note that there are almost no fibers in the adjacent LDTg. Scale bars = 200 μm .



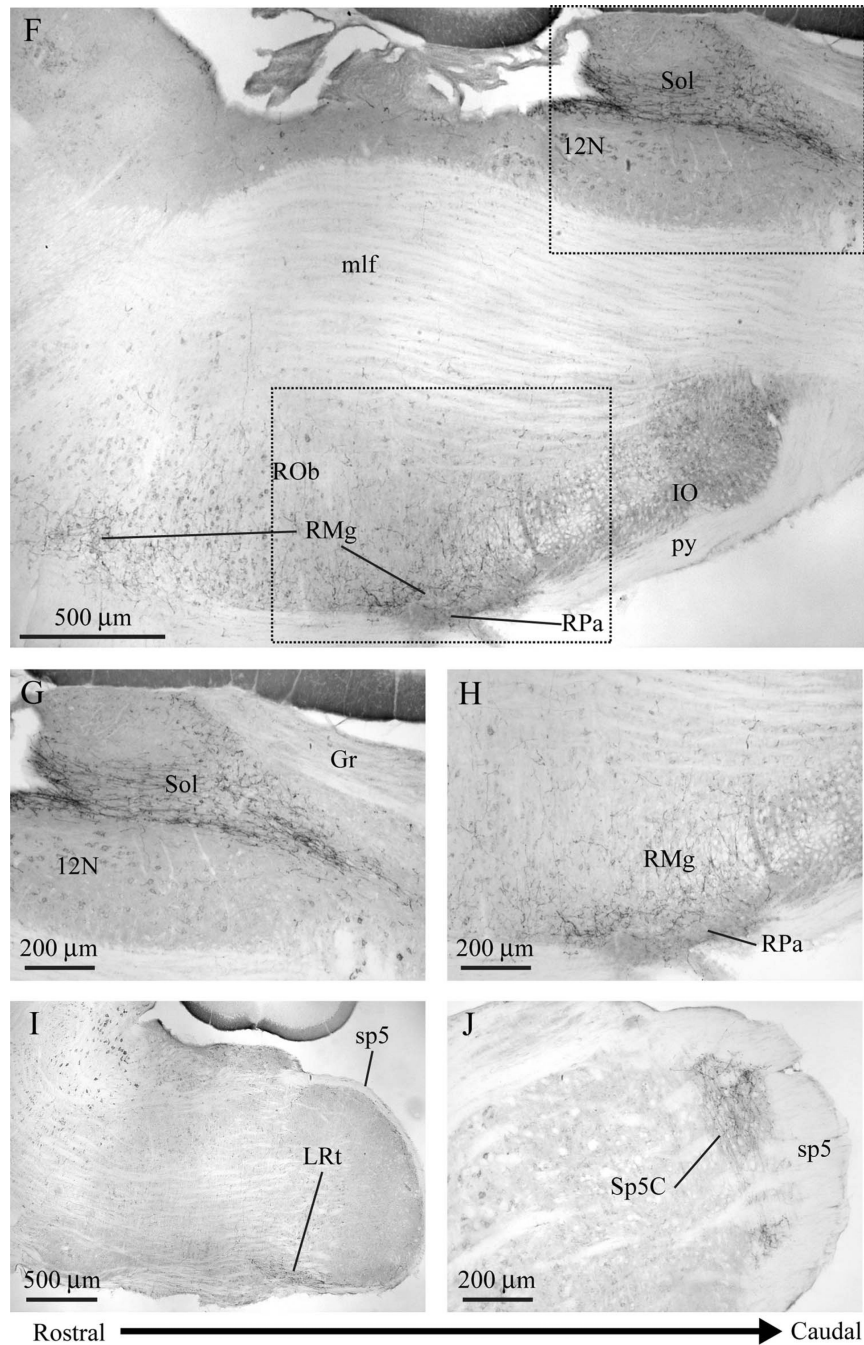
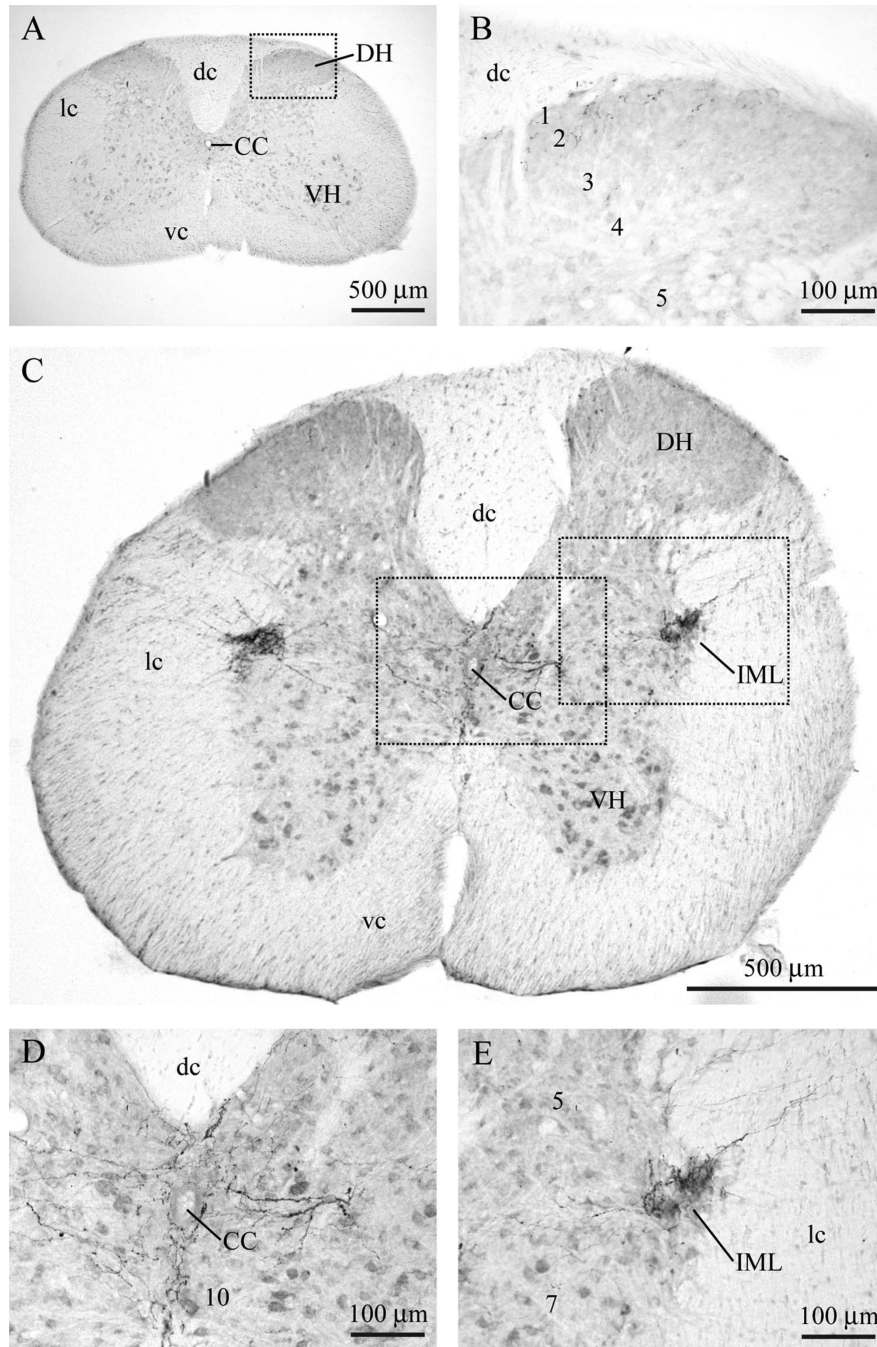


Figure 20.

Metencephalon and myelencephalon. **A:** Bregma -4.36 . Small fibers in the ATg at the intersection of the decussation of the superior cerebellar peduncle (xscp) and the tectospinal tract (ts). **B:** Bregma -4.72 . Small fibers at the midline in the MnR at the level of the pons. **C:** Bregma -5.52 . Medium-sized fibers in the IRt; arrows indicate representative fibers. **D:** Magnification of medium-sized fibers in the Sol from boxed area in E. **E:** Bregma -6.36 . Medium-sized fibers are found in the Sol and in the RMg and GiA. **F:** Lateral -0.04 . Sagittal section near the midline. Dense medium-sized fibers are found in the Sol. Scattered medium-sized fibers are seen in the medullary raphe nuclei, including ROb, RMg, and RPa.

G: Magnification of medium-sized fibers in Sol from top boxed area in F. **H:** Magnification of medium-sized fibers in the raphe nuclei from bottom boxed area in F. **I:** Lateral 1.2. Medium-sized fibers are seen in the LRT. **J:** Lateral 1.56. Medium-sized fibers are seen in the Sp5C. Scale bars = 200 μm in A,D,G,H,J; 100 μm in B; 500 μm in C,E,F,I.



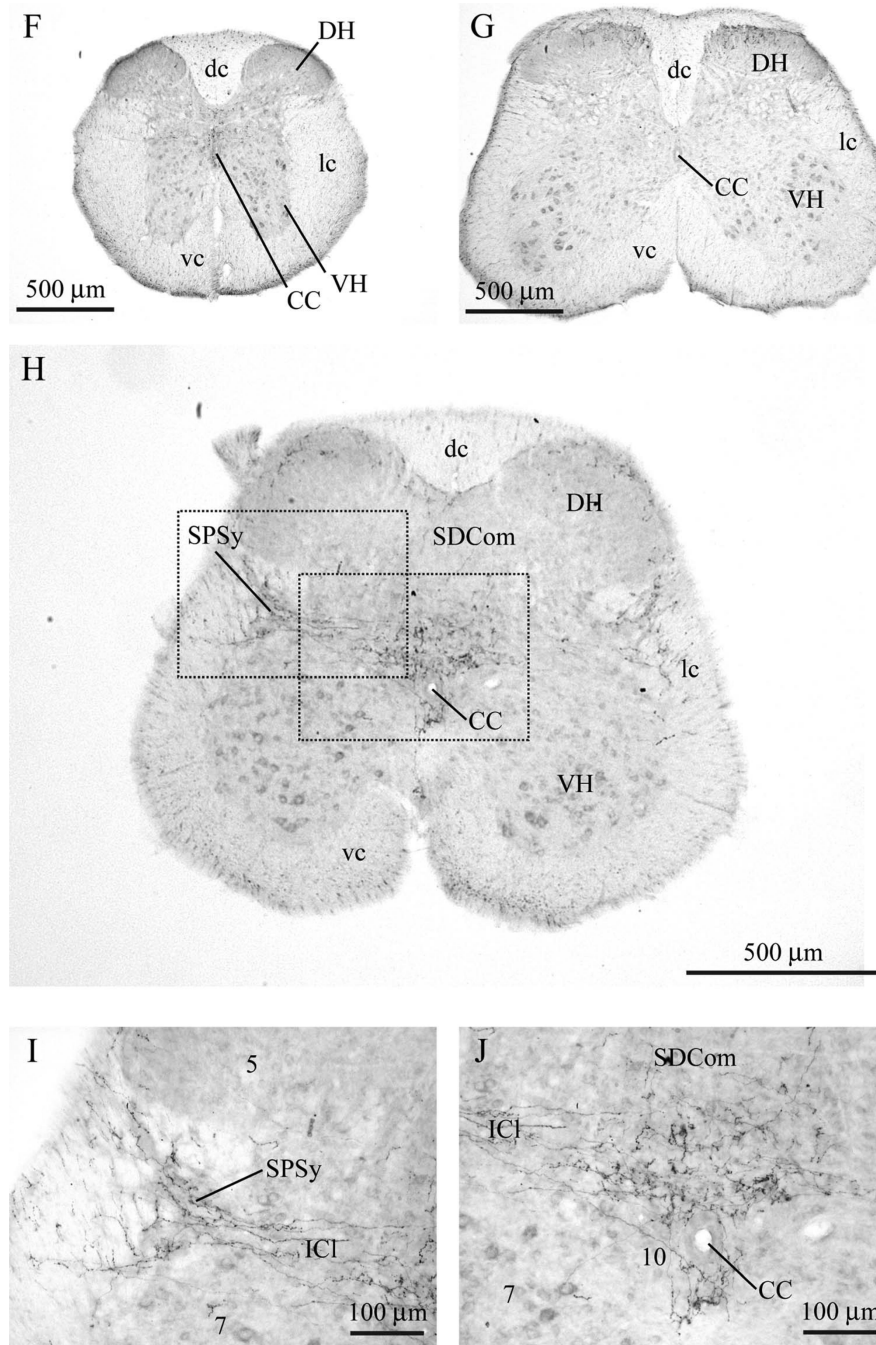


Figure 21.

Spinal cord. **A:** Cervical 6 (approximate segmental location). Sparse to scattered fibers are observed in layer 10 around the CC and layers 1, 2, and 3 of the dorsal horn through most of the cervical spinal cord. **B:** Magnification of medium-sized fibers in dorsal horn from boxed area in A. **C:** Thoracic 1. In the upper thoracic cord, medium-sized fibers increase in layer 10, and some project laterally to the IML. **D:** Magnification of medium-sized fibers around CC from midline box in C. **E:** Magnification of medium-sized fibers in the IML from right box in C. **F:** Thoracic 11. Medium-sized fibers are again found only around the CC and in the dorsal horn in the caudal thoracic cord. **G:** Lumbar 5. more fibers are found in dorsal

horn in the lumbar cord than in other cord regions. **H**: Sacral 1. Moderate medium-sized fibers are found in layer 10 from L6 to S2. Some fibers project laterally into the SPSy. **I**: Magnification of medium-sized fibers in layer 10 and SDCom of the sacral cord from box at midline in H. **J**: Magnification of medium-sized fibers in the SPSy in the sacral cord from left box in H. Scale bars = 500 μm in A,C,F–H; 100 μm in B,D,E,I,J.

TABLE 1

AVP-ir Fiber Density¹

Brain region	Relative density	
	Minimum	Maximum
Telencephalon		
Cortex		
Cingulate cortex (Cg2)	-	+
Dorsal endopiriform nucleus	-	+
Dorsolateral entorhinal cortex (DLEnt)	+	++
Dorsal peduncular cortex	-	+
Ectorhinal cortex	-	+
Frontal cortex	-	+
Infralimbic	-	+
Insular cortex	-	+
Medial orbital cortex	-	+
Piriform cortex (Pir)	-	+
Prelimbic cortex (PrL)	-	+
Ventral endopiriform claustrum	+	++
Hippocampus		
Fimbria	-	+
Lacunosum moleculare (LMol)	+	++
Oriens layer hippocampus (Or)	+	++
Ventral subiculum (VS)	+	++
Basal ganglia		
Nucleus accumbens, core (AcbC)	+	++
Ventral pallidum (VP)	+	++++
Septal complex		
Lateral septal nucleus, dorsal part (LSD)	-	+
Lateral septal nucleus, intermediate part (LSI)	++	++++
Lateral septal nucleus, ventral part (LSV)	++	++++
Rostral lateral septum (LSD, I, & V)	+	++
Septofimbrial nucleus (SF _i)	+	++
Septohypothalamic nucleus (SH _y)	++	+++
Subfornical organ (SFO)	-	+
Triangular septal nucleus	-	+
Ventral forebrain		
Dorsal tenia tecta	+	++
Navicular postolfactory cortex	+	++
Substantia innominata (SI)	+	++++
Ventral septal area (VSA)	+++	++++
Bed nucleus of the stria terminalis		
Anteromedial BNST (BSTMA)	++	+++

Brain region	Relative density	
	Minimum	Maximum
IPAC	-	+
Juxtacapsular BNST	-	+
Laterodorsal BNST	-	+
Lateroposterior BNST	-	+
Lateroventral BNST (BSTLV)	+	++
Medioventral BNST (BSTMV)	++	+++
Posterointermediate BNST (BSTMPI)	++	+++
Nucleus of the stria medullaris (SM)	++	+++
Posterolateral medial BNST (BSTMPL)	++	+++
Posteromedial BNST (BSTMPM)	+++	++++
Amygdala		
Anterior amygdaloid area (AA)	+	++
Anterior cortical amygdala (ACo)	++	+++
Anterodorsal medial amygdala	+++	++++
Anterolateral amygdalohippocampal area	++	+++
Posteromedial amygdalohippocampal area (AHiPM)	+	+++
Anteroventral medial amygdala	+	++
Basomedial amygdala (BMA)	+	++
Basolateral, posterior (BLP)	+	++
Central amygdala (CeA)	-	+
Extended amygdala (EA) ¹	++	+++
Intraamygdalar division of stria terminalis	-	+
IPACM/IPACL	-	+
Posterodorsal medial amygdala (MePD)	+++	++++
Posterolateral cortical amygdala (PLCo)	+	++
Posteroventral medial amygdala	++	+++
Diencephalon		
Hypothalamus: preoptic area		
Anteroventral periventricular Area (AVPe)	++	++++
Lateral preoptic area (LPO)	+	+++
Medial part of medial preoptic nucleus (MPOM)	++	+++
Medial preoptic area (MPA)	++	+++
Median preoptic nucleus (MnPO)	+++	+++
Parastrial nucleus (PS)	+++	++++
Periventricular hypothalamic nucleus (Pe)	++	++++
Striohypothalamic nucleus (StHy)	+	++
Vascular organ of the lamina terminalis (VOLT)	+	++
Ventrolateral preoptic area (VLPO)	+	++
Ventromedial preoptic nucleus (VMPO)	+	++
Hypothalamus: anterior region		
Anterior hypothalamus, anterior (AHA)	+	++++

Brain region	Relative density	
	Minimum	Maximum
Anterior hypothalamus, central (AHC)	+++	++++
Lateroanterior hypothalamus (LA)	+	++
Paraventricular nucleus (PVN)	+++	++++
Parvicellular paraventricular hypothalamus (PaAP)	+++	++++
Periventricular region (Pe)	+++	++++
Retrochiasmatic area	++	++++
Subparaventricular zone (SPa)	+++	++++
Suprachiasmatic nucleus (SCN)	+++	++++
Supraoptic commissure	++	++
Tuberal lateral hypothalamus (TuLH)	+++	++++
Hypothalamus: mammillary body	Min	Max
Dorsal hypothalamic area	-	+
Dorsal tuberomammillary nucleus (DTM)	+++	++++
Endopeduncular nucleus	+	++
Lateral retromammillary nucleus	+	++
Medial retromammillary nucleus (RMM)	+	++
Perifornical nucleus	+++	++++
Posterior hypothalamus (PH)	+	++
Ventral premammillary nucleus (PMV)	+	++
Ventral tuberomammillary nucleus (VTM)	+++	++++
Hypothalamus: dorsomedial region		
Arcuate nucleus (Arc)	+	++
Dorsomedial hypothalamus (DMH)	++	++++
Medial tuberal hypothalamus	+	++++
Ventromedial hypothalamus (VMH)	-	+
Zona incerta (ZI)	-	+
Hypothalamus: lateral region		
Lateral hypothalamus (LH)	++	++++
Peduncular part of the lateral hypothalamus (PLH)	+++	++++
Perifornical lateral hypothalamus (PeFLH)	+++	++++
Thalamus		
Central medial thalamic nucleus (CM)	++	+++
Interanterodorsal thalamic nucleus (IAD)	++	+++
Interanteromedial thalamic nucleus (IAM)	++	+++
Lateral habenular nucleus (LHb)	++	++++
Mediodorsal thalamic nucleus (MD)	+++	++++
Paracentral thalamus (PC)	++	+++
Paratenial thalamus (PT)	+	++
Paraventricular thalamic n., anterior (PVA)	++	++++
Paraventricular thalamic nucleus, middle (PV)	++	+++
Paraventricular thalamic n., posterior	+	++

Brain region	Relative density	
	Minimum	Maximum
Reticular nucleus	-	+
Reuniens thalamic nucleus (Re)	+	++
Rhomboid thalamic nucleus (Rh)	+	++
Xiphoid nucleus (Xi)	++	+++
Mesencephalon		
PAG and dorsal raphe		
Commissure of the superior colliculus (csc)	+	++
Dorsal raphe, caudal (DRC)	+	+++
Dorsal raphe, dorsal (DRD)	+	++++
Dorsal raphe, interfascicular (DRI)	+	++
Dorsal raphe, ventral	+	++
Dorsolateral PAG	+	++
Dorsomedial PAG (DMPAG)	+++	++++
Lateral PAG	+	++
Periaqueductal gray, rostral (PAG)	+	++
Ventrolateral dorsal raphe (DRL)	+++	++++
Ventrolateral PAG (VLPAG)	++	++++
Tegmentum		
Barrington's nucleus (Bar)	++	+++
Caudal linear raphe (CLi)	+	+++
Interfascicular nucleus (IF)	++	++++
Lateral parabrachial (LPB)	++	+++
Locus coeruleus (LC)	+	+++
Medial parabrachial (MPB)	+	++
Medial retromammillary nucleus (RMM)	+	++
Midbrain reticular formation (mRt)	+	++
Parabrachial pigmented n. of the VTA (PBP)	+	++
Parainterfascicular nucleus (PIF)	+	++++
Parasubthalamic nucleus (PSTh)	+	++
Peripeduncular nucleus	-	+
Retrorubral field (RRF)	+	+++
Rostral linear raphe	-	+
Substantia nigra pars compacta (SNC)	++	+++
Substantia nigra, lateral part	++	+++
Substantia nigra pars reticulata (SNR)	+	++
Subthalamic nucleus	-	+
Ventral tegmental area (VTA)	++	+++
Zona incerta (ZI)	+	++
Metencephalon		
Anterior tegmental nucleus (ATg)	+	++
Median raphe (MnR)	+	++

Brain region	Relative density	
	Minimum	Maximum
Myelencephalon		
Gigantocellular reticular n., alpha part (GiA)	+	++
Gigantocellular reticular n., ventral part	+	++
Intermediate reticular formation (IRt)	+	++
Lateral reticular n. (LRt)	+	+++
Parvicellular reticular n., alpha part	-	+
Raphe interpositus nucleus	-	+
Raphe magnus nucleus (RMg)	+	++
Raphe obscurus nucleus (ROb)	-	+
Raphe pallidus nucleus (RPa)	+	++
Spinal trigeminal n., caudal part (Sp5C)	+	+++
Solitary nucleus (Sol)	++	++++
Subcoeruleus nuclei	-	+
Supermedullary vellum	-	+

Abbreviations are listed only for those areas mentioned elsewhere in the text. -, No AVP-ir fibers; +, sparse; ++, scattered; +++, moderate; and ++++, dense.

¹ Areas where AVP immunoreactivity was detected. The minimum and maximum values indicate the range of density in individual areas.